



Riverine nitrogen supply to the global ocean and its limited impact on global marine primary production: a feedback study using an Earth System Model

Miriam Tivig¹, David P. Keller¹, and Andreas Oschlies¹

¹GEOMAR Helmholtz-Zentrum für Ozeanforschung Kiel, Düsternbrooker Weg 20, 24105 Kiel, Germany

Correspondence: Miriam Tivig (mtivig@geomar.de)

Abstract. A common notion is that negative feedbacks stabilize the marine nitrogen inventory. Recent modeling studies have shown, however, some potential for localized positive feedbacks leading to substantial nitrogen losses, in regions where nitrogen fixation and denitrification occur in proximity to each other. Here we include dissolved nitrogen from river discharge in a global 3-D ocean biogeochemistry model and study the effects on near-coastal and remote open ocean biogeochemistry. We find that at steady state the biogeochemical feedbacks in the marine nitrogen cycle, nitrogen input from biological N₂ fixation, and nitrogen loss via denitrification, mostly compensate for the yearly addition of 22.8 to 45.6 Tg of riverine nitrogen and limit the impact on global marine productivity to < 2 %. Global experiments that regionally isolate river nutrient input show that sign and strength of the feedbacks depend on the location of the river discharge and the oxygen status of the receiving marine environment. Marine productivity generally increases in proximity to the nitrogen input, but we also find a decline in productivity in the Bay of Bengal and near the mouth of the Amazon River. While most of the changes are located in shelf and near coastal oceans, nitrogen supply from the rivers can impact the open ocean, due to feedbacks or knock-on effects.

1 Introduction

Nitrogen plays a key role in marine biogeochemistry in coastal and open oceans, as it is one of the major limiting nutrients for algal photosynthesis. Variations in the oceanic fixed-nitrogen (N) inventory are known to have driven marine productivity changes contributing to atmospheric CO₂ variations in Earth's history (Falkowski, 1997).

Although several studies questioned the stability of the global N budget (Codispoti et al., 2001; Gruber and Sarmiento, 1997; Codispoti, 1995), the present marine N inventory is generally considered to be in steady state (Deutsch et al., 2007; Altabet, 2006; Gruber, 2004; Tyrrell, 1999; Redfield et al., 1963). Oceanic fixed nitrogen concentrations are mainly controlled by the balance between denitrification and N fixation, creating negative feedbacks which damp the often strong variations of the marine N content with respect to the more slowly overturning phosphorus (P) inventory (Somes et al., 2013; Deutsch et al., 2007; Gruber, 2004; Ruttenger, 2003).



In regions where fixed N is sparse, organisms that fix atmospheric nitrogen (N_2), commonly called diazotrophs, can compensate N deficits (Deutsch et al., 2007, 2001; Capone et al., 1997). As diazotrophs consume phosphate while adding N to their environment, they are generally considered to regulate their own population. In regions where N is more abundant, the slowly growing diazotrophs are, according to current model concepts, rapidly out-competed by non-fixing organisms, if enough P and other nutrients are present (Tyrrell, 1999).

Denitrification is a metabolic process in which nitrate (NO_3) replaces oxygen (O_2) as terminal electron acceptor for respiration and is reduced to N_2 , which is not bioavailable for most marine organisms (Gruber, 2004; Deutsch et al., 2001). Denitrification represents the main sink for fixed N in the ocean and occurs both in marine sediments and in the water columns under suboxic conditions (Gruber, 2004; Codispoti et al., 2001). But denitrification limits itself by reducing the concentrations in fixed N at the surface, which in turn limits the growth of phytoplankton and the consumption of O_2 , eventually making NO_3 less competitive as electron acceptor, where O_2 remains available (Landolfi et al., 2013; Gruber, 2004). These two processes, N_2 fixation and denitrification, work together to regulate the global marine N budget.

Beside the fixation of atmospheric N_2 , rivers are also a major source of N to the coastal and the open ocean. Rivers are estimated to add 36-60 Tg $N\ yr^{-1}$ to the coastal waters (Beusen et al., 2016; Mayorga et al., 2010; Seitzinger et al., 2005). These N inputs are regionally highly diverse and range over several orders of magnitude (Meybeck et al., 2006). Other sources of N include atmospheric deposition, which will not be considered in this study.

Although riverine N is not the main source of N to the marine environments, it can become a key player, as it is highly influenced by human activities (Seitzinger et al., 2010; Smith et al., 2003; Rabelais et al., 2002) and is known to impact coastal marine biology and biogeochemistry, leading for example to eutrophication, algal blooms or hypoxia (e.g. Seitzinger et al., 2010; Billen and Garnier, 2007; Smith et al., 2003). Previous studies have shown, that nutrient input from land also has consequences for sea water composition and by this impacts biogeochemical processes in the open ocean farer away from the coasts (e.g. Barron and Duarte, 2015; Bauer et al., 2013; Bernard et al., 2011; Jahnke, 2010).

As global measurements of N concentrations and fluxes are difficult, models are often used to study the marine N cycle and its feedbacks. However, current global biogeochemical ocean models still often omit riverine nutrient input to the ocean or represent it in a very simplified form. Giraud et al. (2008) for example, tested the sensitivity of the global ocean biogeochemistry to coastal nutrient fluxes in a global ocean biogeochemistry model by introducing nutrients in different scenarios in the coastal grid boxes. They found that excess nutrients in the coastal ocean could impact the biological activity not only locally but also in the open ocean and that the effect depended more on the ratio between these nutrients and iron and silicate, as on the actual quantities. Nevertheless, the study by Giraud et al. (2008) was an idealized experiment without real nutrient fluxes and a relatively simple representation of the ecosystem dynamics, where total nitrogen nutrient and phosphate were linked by Redfield ratio and indifferently represented by one model variable. Da Cunha et al. (2007) used an ocean biogeochemistry model to analyze the impact of river nutrient fluxes (N, Si, Fe and Carbon) on the global and coastal ocean primary production, but concentrated on a short time period of a few decades, likely not long enough to study the feedbacks of the nitrogen cycle in the open ocean.

More recently, Lacroix et al. (2020) implemented estimations of riverine nutrient loads in a global ocean model to analyze their



implications for global oceanic nutrient concentrations, primary production and CO₂ fluxes. Their focus was on pre-industrial nutrient export estimated as a function of precipitation, surface runoff and temperature. N was calculated from the simulated P
60 using a fixed N:P ratio, but Lacroix et al. (2020) did not analyze the N cycle feedbacks.

For our study, we used the Earth system climate model of intermediate complexity of the University of Victoria (UVic, Version 2.9, Eby et al. (2009); Weaver et al. (2001)). Earth System Models of Intermediate Complexity (EMICs) have been developed to fill the gap between more abstract conceptual models and comprehensive global and Earth system models (ESM) (Claussen et al., 2002). EMICs allow the integration of a large number of processes, more than conceptual models, using often coarser
65 resolution and simplifying assumptions e.g. describing the atmospheric circulation compared to ESMs. UVic has been developed as a tool helping to understand processes and feedbacks operating within the climate system on decadal and longer timescales (Weaver et al., 2001).

Previously, Landolfi et al. (2017) and Somes et al. (2016) used UVic to study the response of the marine N cycle to idealized atmospheric N deposition and its impact on marine productivity. Both found that N cycle feedbacks stabilize the model's marine N inventory and limit changes to the marine N cycle and productivity.
70

Here, we again use UVic, but without atmospheric N deposition, to focus on the marine biogeochemical response to riverine N inputs to the coastal ocean. To do this we make use of modeled estimates of riverine DIN export from watersheds (Mayorga et al., 2010). While atmospheric deposition is more spread out over the whole ocean, river export of dissolved N reaches the ocean as point sources at different locations and in different concentrations. The global amount of N added to the ocean is
75 comparable between our river-supply study and the atmospheric supply ones by Somes et al. (2016) and Landolfi et al. (2017). Nevertheless, we hypothesize that the response of the marine ecosystem differs with highly concentrated nutrient injections associated with individual rivers.

To test the mechanisms and feedbacks described in the two previous studies (Landolfi et al., 2017; Somes et al., 2016) but now with river nitrogen fluxes, we perform a series of simulations with different amounts of N input. Analogous to earlier studies
80 (Lacroix et al., 2020; Da Cunha et al., 2007), we first evaluate the global N inventory and marine primary production after sustained addition of riverine DIN. In a second step, we additionally performed a series of experiments, where we study the responses of the ocean to riverine nutrient supply from individual regions.

2 Model description and experimental design

Nutrients from the Global Nutrient Export from Water-Sheds (NEWS) 2 model (Mayorga et al., 2010) are added to the University of Victoria Earth System Climate Model (UVic) 2.9 (Keller et al., 2012; Eby et al., 2009; Weaver et al., 2001). The model is outlined, before describing the NEWS2 data set and our experimental design below.

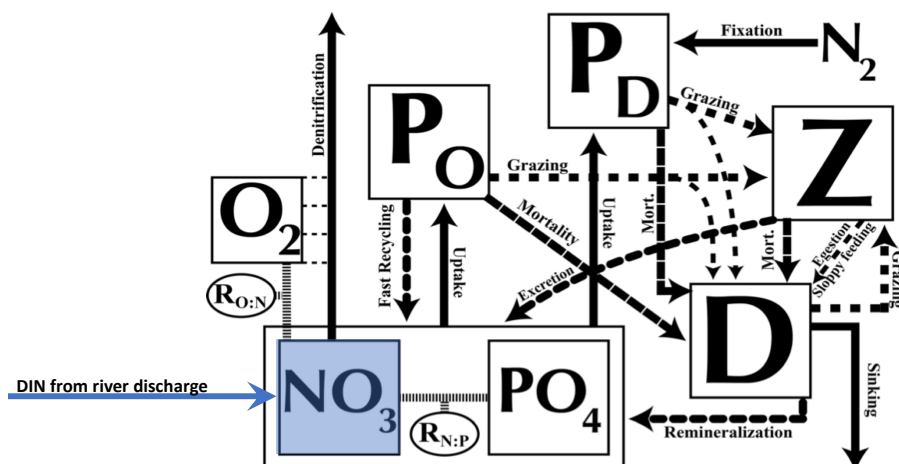


Figure 1. Ecosystem model schematics for the NPZD model with the prognostic variables (in square boxes) and the fluxes of material between them, indicated by arrows. See details in the text. Figure updated from Keller et al. (2012).

2.1 The Earth System Model UVic 2.9

UVic (Weaver et al., 2001) version 2.9 (Keller et al., 2012; Eby et al., 2009) is an Earth System Model of intermediate
 90 complexity (Claussen et al., 2002). It consists of a three-dimensional ($1.8^\circ \times 3.6^\circ$, 19 levels) general circulation model of the ocean, a two-dimensional, single-layer energy-moisture balance atmospheric model, a dynamic-thermodynamic sea ice model, and a terrestrial vegetation model.

The atmospheric component dynamically calculates heat and water fluxes between the atmosphere and the ocean, land and sea ice, and is forced by monthly climatological winds prescribed from NCEP/NCAR. The nineteen vertical levels of the oceanic
 95 component, Modular Ocean Model 2 (MOM2), are 50 m thick near the surface and up to 500 m in the deep ocean. The oceanic physical settings are the same as in Keller et al. (2012). The marine ecosystem module of UVic is based on Keller et al. (2012) with updates as noted in Partanen et al. (2016). Seven prognostic variables are embedded within the ocean circulation: two phytoplankton classes (nitrogen fixing diazotrophs and other phytoplankton), zooplankton, sinking particulate detritus, nitrate (NO_3), phosphate (PO_4) and oxygen (O_2) (Fig. 1). All biological variables as well as the detritus are expressed in terms of
 100 nitrogen (mmol N m^{-3}), using Redfield stoichiometry to calculate C:N and N:P ratios. Since diazotrophs can fix atmospheric N, they are not limited by NO_3 concentrations, while the growth of other phytoplankton is limited by NO_3 and PO_4 (note that both are additionally limited by iron, light and temperature). See Keller et al. (2012) for a full description and evaluation of simulated marine biogeochemistry.



In the global ocean, fixed N is regulated by the major input fluxes, N_2 fixation and riverine input, and the major removal
105 flux, denitrification (here implicitly including anammox). Benthic denitrification, in particular, is believed to be the major sink
for fixed N (Voss et al., 2013; Galloway et al., 2004). It is included here through empirical transfer functions derived from
benthic flux measurements (Bohlen et al., 2012). The functions are based on dynamic vertically integrated sediment models
and estimate denitrification from the rain rate of particulate organic carbon to the seafloor and bottom water O_2 and NO_3
concentrations. Like Somes and Oschlies (2015) and Somes et al. (2013) we use a subgrid bathymetry scheme for shallow
110 continental shelves and other topographical features that are too fine to be resolved on the coarse UVic grid, in order to better
resolve particulate organic matter sinking and remineralization at the seafloor.

2.2 Including riverine nutrient supply to the UVic ocean

2.2.1 Global Nutrient Export from WaterSheds 2 : NEWS2

Riverine N added to UVic has been generated by a global, spatially explicit model of nutrient exports by rivers. NEWS2
115 (Mayorga et al., 2010) is the second version of a system of sub-models, which estimate present-day annual export yield for
each river basins ($kg\ N\ km^{-2}\ yr^{-1}$) at the river mouths for dissolved and particulate forms of organic and inorganic N and P,
as well as dissolved organic and particulate carbon. See Mayorga et al. (2010) for more details on the model configuration.
Each sub-model predicts river export of a nutrient element for the base year 2000. This export is calculated as a function of
natural and anthropogenic biogeophysical properties of each of the 5761 exoreic basins considered (Seitzinger et al., 2005).
120 NEWS-DIN includes DIN from sewage point sources, as well as N from diffuse sources, mobilized from watershed soils and
sediments (Dumont et al., 2005). Despite uncertainties and errors, NEWS-DIN predicts 54-78 % of the variability in DIN
export yield ($kg\ N\ km^{-2}\ yr^{-1}$) and 72-83 % of DIN export load ($kg\ N\ basin^{-1}\ yr^{-1}$) of the validation data set used by Dumont
et al. (2005).

2.2.2 NEWS-DIN for UVic

125 To estimate total export per river mouth, we multiplied the yields ($kg\ N\ km^{-2}\ yr^{-1}$) of DIN and dissolved organic nitrogen
(DON) by the respective basin area (in km^2). Data from the NEWS2 models have been interpolated on the coarser UVic grid
and the total exports per river basins have been added to the nearest discharge points, as not every river mouth from NEWS2
has its equivalent discharge point in UVic (Fig. 2). Because there can be strong seasonal variations in nutrient fluxes and
fluvial nutrient imports can have different effects on the biogeochemistry of a coastal ecosystem depending on the timing of
130 the fluxes (Eisele and Kerimoglu, 2015; Holmes et al., 2012; Townsend-Small et al., 2011), we used the seasonally cycling
climatology of freshwater runoff from UVic to estimate seasonal variations in N supply. Although freshwater discharge and
riverine nutrients export are not always correlated, the discharge has an important impact on the nutrient loads of rivers (e.g.
Lu et al., 2011, 2009; Sigleo and Frick, 2007; DeMaster and Pope, 1996). Here, we assumed that nitrogen concentrations in the
discharged river water are constant throughout the seasonal cycle and distributed the annual load over the months, weighted by
135 the fraction of monthly freshwater discharge.

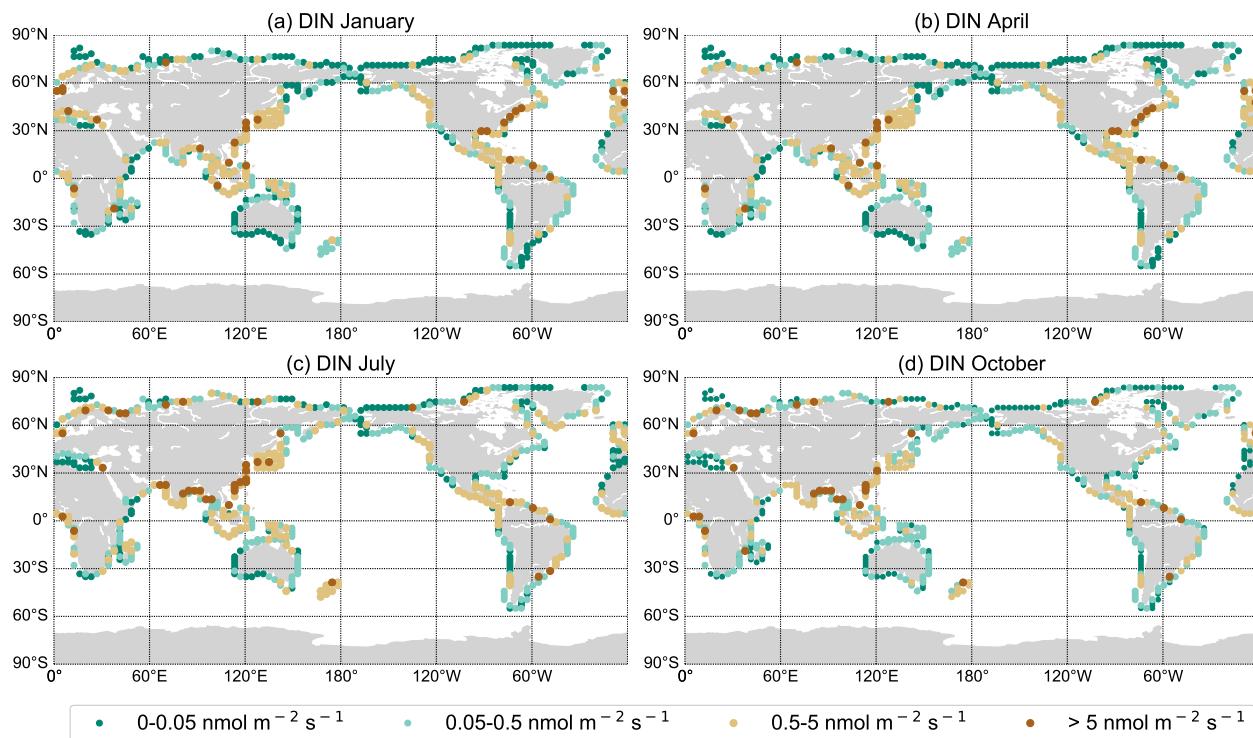


Figure 2. DIN export yield for each discharge point in $\text{nmol m}^{-2} \text{s}^{-1}$ from NEWS2 data set interpolated on the UVic grid for January (a), April (b), July (c) and October (d).

2.3 Experimental design

To analyze the effect of riverine nutrient export in the UVic model, three experiments have been performed (Table 1). All simulations were run for 10000 years with benthic denitrification and subgrid bathymetry, starting from an already spun-up steady state with the standard model version (i.e., with no riverine nutrient input) with pre-industrial conditions for insolation and a fixed atmospheric CO_2 concentration of 283 ppm (Keller et al., 2012). In NEWS only DIN from NEWS2 (NEWS-DIN) was added to the discharge points in UVic. In DIN+DON we added DIN and DON from NEWS2 (NEWS-DIN and NEWS-DON). In 2xDIN twice the yield of DIN from NEWS-DIN has been added. For comparison, a control simulation has been run for 10000 years without riverine DIN supply (referred to as CTR). Globally, NEWS2 predicts a riverine N supply of 22.8 Tg N yr^{-1} for DIN and 11.8 Tg N yr^{-1} for DON. Both enter the biogeochemical model as NO_3 fluxes in $\text{mol N m}^{-2} \text{s}^{-1}$, thereby implicitly assuming that all DON is bioavailable. The marine ecosystem dynamics as well as the biogeochemical cycles of the model run have been evaluated in previous studies under the standard boundary conditions, without riverine nutrients (e.g. Somes et al., 2013; Keller et al., 2012; Somes et al., 2010b; Schmittner et al., 2008, 2005). We therefore concentrate on the evaluation of the response of the marine biogeochemical model to the new model component of riverine nutrient discharge. At



Table 1. Global annual nutrient flux from river discharge from Global Nutrient Export from WaterSheds 2 (Mayorga et al., 2010)

Simulation	Global N-flux [Tg N yr ⁻¹]	Short description
UVic NEWS	22.8	Riverine DIN input from NEWS2
UVic DIN+DON	34.6	Riverine DIN + DON input from NEWS2
UVic 2xDIN	45.6	Twice the riverine DIN input from NEWS2

the end of all simulations, the N budget reached a steady state. For the evaluation of the resulting ocean biogeochemistry, we
150 analyze in the following the mean of the last 100 years of each simulation.

3 Results

3.1 Nitrogen

3.1.1 Global nitrate distribution

In comparison with observational data of the World Ocean Atlas (Garcia et al., 2019), the model simulates the observed NO₃
155 profiles fairly well (Fig. 3). UVic underestimates the NO₃ concentration in the subsurface waters globally and in each ocean
basin by 3 to 4 mmol m⁻³. Global average NO₃ concentrations only vary a little between the simulations, but the misfit between
model and observations decreases with higher riverine N supply (top right panel in Fig. 3). At the surface, the global ocean
NO₃ distribution patterns are very similar between the model and the observations, as well as between the control (CTR) and
the NEWS simulation (Fig. 4).

160 Nevertheless, at smaller scale, in all three simulations (NEWS, DIN+DON, and 2xDIN), NO₃ concentrations are globally
higher compared to the control simulation (CTR) (Fig. 5, Fig. 6). The supply of riverine NO₃ affects the ocean nutrient
concentration not only locally near the river mouths, but also in regions far away from the coasts. Surface NO₃ concentrations
increase with higher river supply in the coastal regions and in the higher latitudes. The globally highest increase in NO₃ can
be found in the 2xDIN experiment (see also table 2) and the NO₃ increase is higher in the deeper ocean than at the surface.
165 Interestingly, the increase in the oceanic N inventory is more than twice as high in UVic 2xDIN compared to UVic NEWS,
indicating non-linear feedbacks.

While higher NO₃ concentrations due to riverine input are not surprising, some regions present however lower concentrations
compared to CTR. In all simulations NO₃ is slightly lower at the surface in large parts of the tropical and subtropical oceans.
At 300 m depth and even more at 850 m depth, the ocean loses NO₃ upon the addition of riverine N in our simulations in low
170 oxygen regions where denitrification occurs, in the Gulf of Benguela, the Bay of Bengal and the eastern equatorial Pacific near
the coast of Central America (Fig. 6).

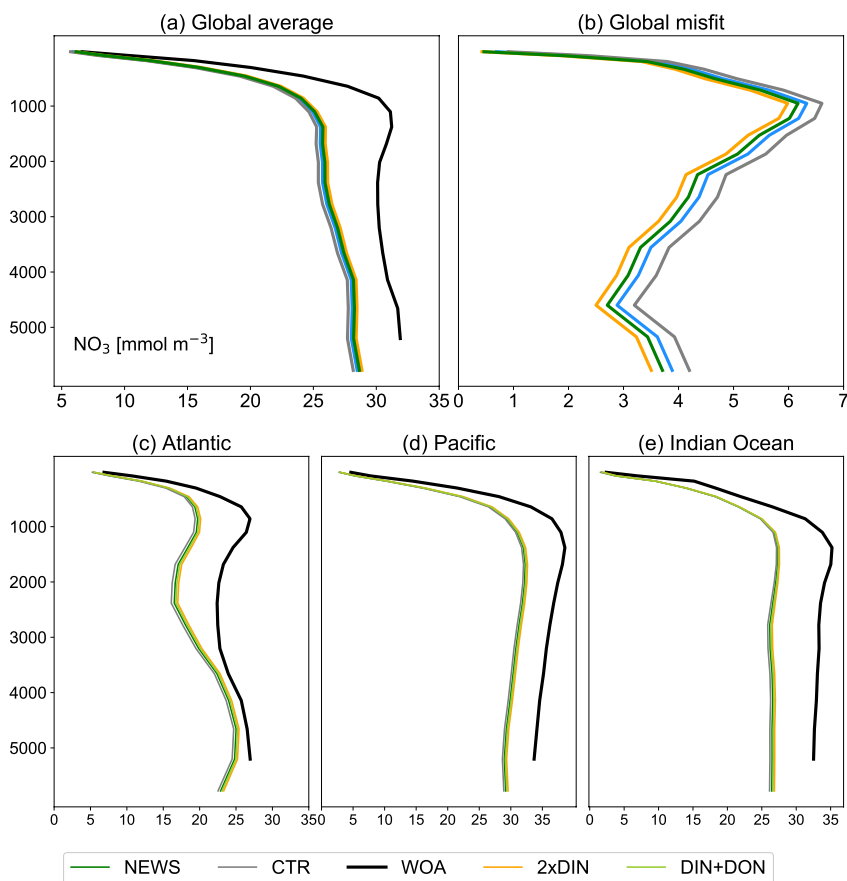


Figure 3. Profiles of global averaged NO₃ in mmol m⁻³ from UVic simulations with and without riverine DIN export from NEWS data sets and observations with the WOA. (a) Global ocean average of NO₃. (b) Global profiles of misfit in NO₃ compared to the observations. (c)-(e). NO₃ profiles for the three main ocean basins, Atlantic (ATL), Pacific (PAC) and Indian Ocean (IND).

Table 2. Amount of additional nitrogen in Tg N at the end of each simulation compared to CTR

Simulation	Total N added in 10000 yrs of simulation	Change in N inventory	Relative change in N inventory
	[Pg N]	[Tg N]	[%]
UVic NEWS	228	5278	+ 1,12
UVic DIN+DON	346	8298	+ 1.77
UVic 2xDIN	456	11895	+ 2.53

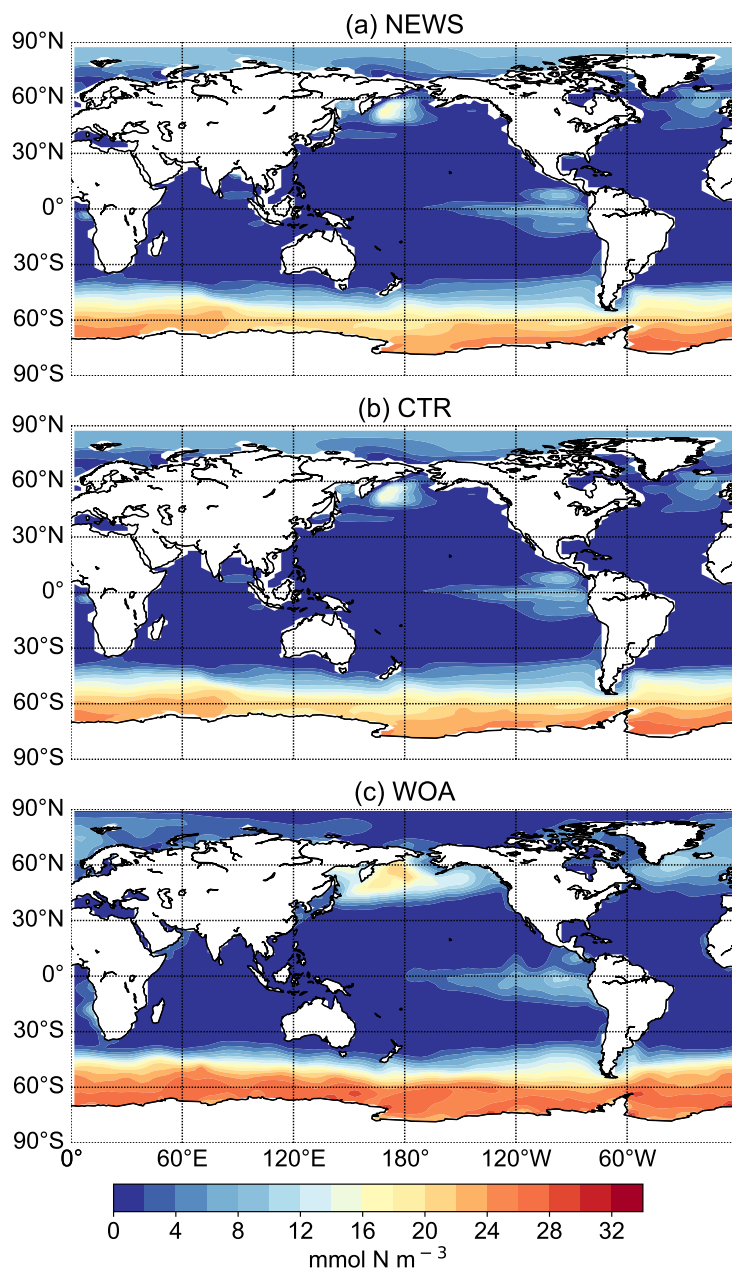


Figure 4. Surface NO₃ concentrations for simulations UVic NEWS (a), UVic control (b) and from observations from World Ocean Atlas (Garcia et al., 2019) (c).

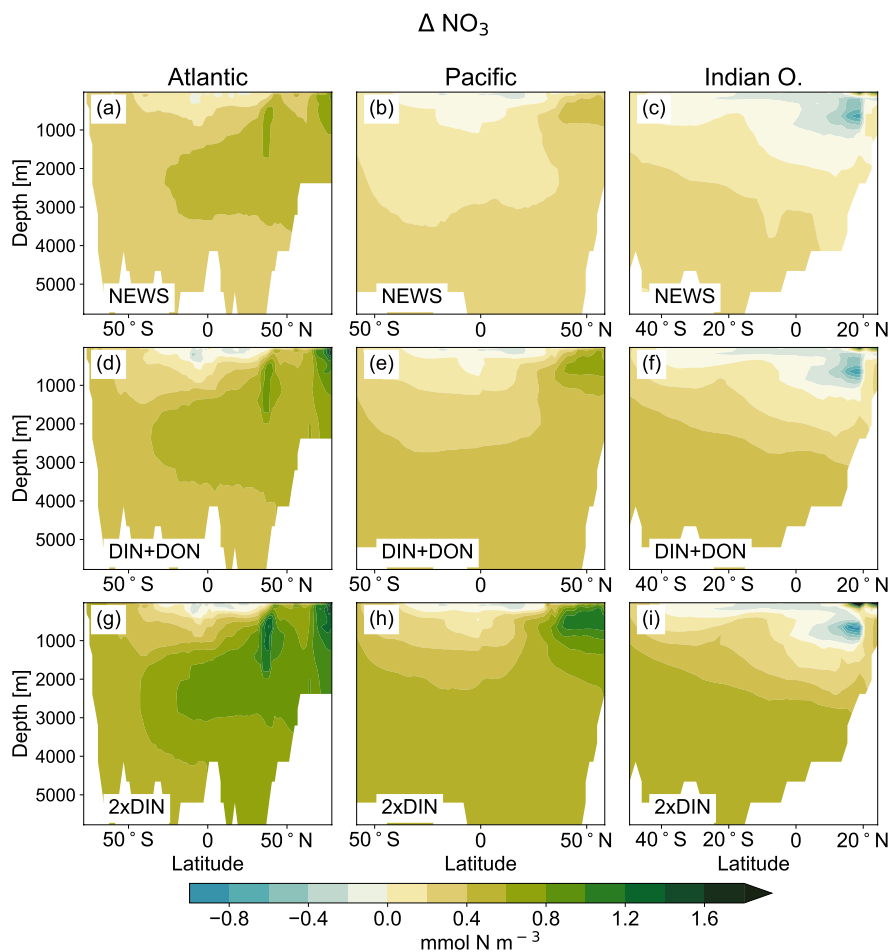


Figure 5. Difference in zonal mean ocean concentrations of NO_3 between the UVic simulations with riverine DIN export and the control simulation. a,b,c : difference between NEWS and CTR; d,e,f : difference between DIN+DON and CTR; g,h,i : difference between 2xDIN and CTR. The columns show the zonal mean of the Atlantic (a,d,g), the Pacific (b,e,h) and the Indian Ocean basins (c,f,i). The difference in zonal averaged NO_3 concentrations are higher than the colorbar maximum at the surface in the northern Indian Ocean basin with a maximum for 2xDIN at $7.2 \text{ mmol N m}^{-3}$.

In major parts of the Atlantic and Pacific Ocean basins, NO_3 concentrations are higher in NEWS than in CTR (Fig. 5). NO_3 is particularly elevated in the upper 2000 m in the North Atlantic Ocean (up to 2 mmol N m^{-3} in 2xDIN, corresponding to +18 %) and upper 1000 m in the North Pacific, but the difference between the simulations is positive in the whole basins, indicating that a substantial part of the additional riverine N is exported into the open and deeper ocean. At the surface of the tropical and subtropical oceans, however, NO_3 concentrations are lower by maximal $-0.9 \text{ mmol N m}^{-3}$ in the UVic-NEWS experiments compared to CTR.

175

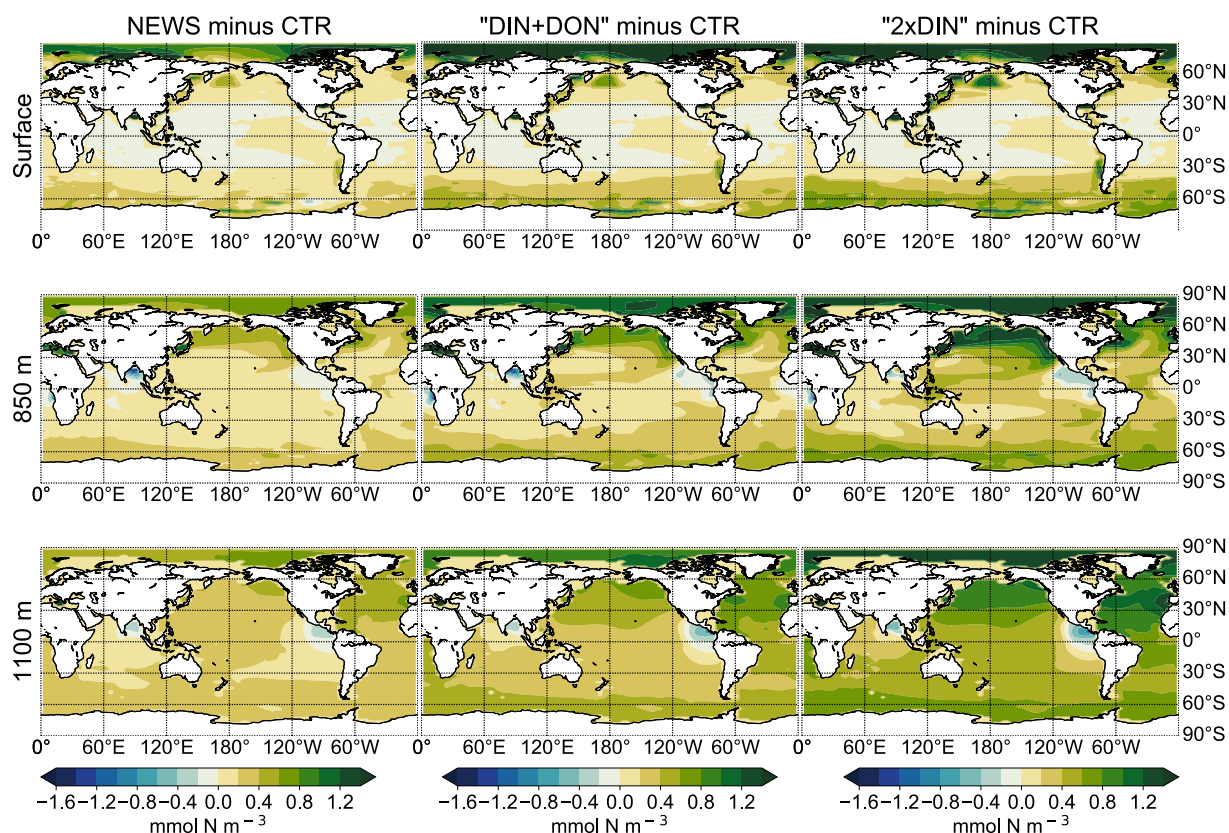


Figure 6. Difference in global distribution of NO_3 concentrations between experimental simulation and the control simulation in mmol N m^{-3} ; The different simulations are NEWS, DIN+DON and 2xDIN. The differences are shown at three different depths: Surface (top), 300 m (middle) and 850 m (bottom).

The Indian Ocean basin comprises the Arabian Sea and the Gulf of Bengal. Zonally averaged NO_3 concentrations reflect essentially the behavior of the Bay of Bengal, where the rivers of the Ganges Delta supply high amounts of nutrients to the northern basin (Fig. 5, Fig. 7). Here, the model simulates high NO_3 concentrations at the surface (in the north, several hundred percent higher in NEWS when compared to CTR). But underneath in the northern Indian Ocean basin down to approximately 2000 m, NO_3 concentrations are significantly lower in NEWS than in CTR (considering the zonal average of the Indian Ocean by -0.7 to $-0.9 \text{ mmol N m}^{-3}$, more if only the zonal average of the Bay of Bengal is considered).

Part of the global NO_3 patterns can be explained by the interaction of ocean circulation and biology. N is transported into the interior ocean via circulation and also accumulates due to the biological pump. But these processes do not explain the loss in N in the subtropical surface oceans or the Bay of Bengal. The same applies to the total amounts of N. Despite the continuous



NEWS minus CTR

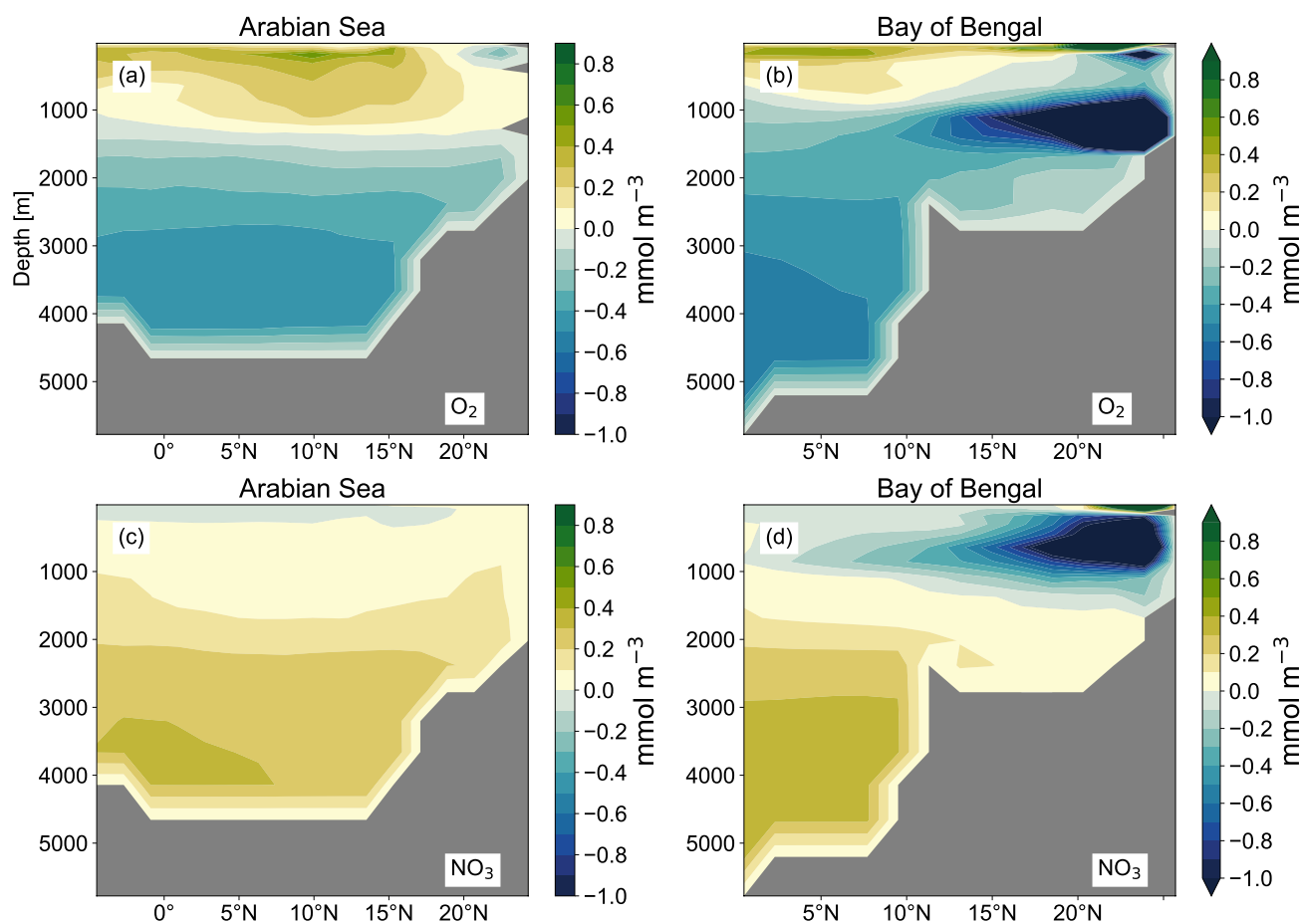


Figure 7. Zonal average of NO_3 and O_2 in the basins of the Arabian Sea (a, c) and the Gulf of Bengal (b, d). All panels show the difference between CTR and NEWS simulations in mmol m^{-3} . In the Bay of Bengal, extreme differences in zonal averaged O_2 concentrations are -4.2 mmol m^{-3} and $+2.1 \text{ mmol m}^{-3}$, in zonal averaged NO_3 concentrations -2.4 mmol m^{-3} and $+7.6 \text{ mmol m}^{-3}$.

supply from the rivers, the additional NO_3 in NEWS, DIN+DON and 2xDIN compared to CTR amounts only to 1.1 %, 1.8 % and 2.5 %, respectively (Table 2). What limits the increase in the global oceanic N inventory is the combination of the N cycle processes denitrification and N_2 fixation.



190 3.1.2 Feedback mechanisms: denitrification and nitrogen fixation

Denitrification is known to be the main sink for fixed N in the ocean (Gruber, 2004; Codispoti et al., 2001). It occurs both in marine sediments and in the water columns under suboxic conditions, like for example in the simulated Bay of Bengal. As a result of these dynamics, if N is added via river discharge, UVic simulates higher water column and benthic denitrification rates (Table 3).

195 At the same time, total global N₂ fixation rates decrease in all three simulations compared to CTR (Table 3). Nitrogen fixation is a significant process in the marine nitrogen cycle and a major source of nitrogen in the open ocean. Nitrogen fixing organisms are able to convert dissolved nitrogen gas (N₂) into ammonia, but are limited in their growth by phosphate and iron (Deutsch et al., 2007; Moore and Doney, 2007; Karl et al., 1997; Redfield et al., 1963). The global rate and geographical distribution of nitrogen fixation are still uncertain. Observations remain sparse and highly variable in space and time. Combined with in-
200 sufficient understanding of the controls of marine N₂ fixation, this results in high uncertainties in the global pattern of marine nitrogen fixation (Wang et al., 2019; Landolfi et al., 2018; Somes et al., 2013). Deutsch et al. (2007) and Luo et al. (2012) estimated a global nitrogen fixation rate of 140 Tg N yr⁻¹ and most recent studies stay in this range, although some studies suggest, that the global rates could be much higher (Wang et al., 2019; Landolfi et al., 2018; Somes et al., 2013; Karl et al., 2002).

205 The global rates calculated from our experiments with UVic (Table 3) are also higher than the estimates from Deutsch et al. (2007) and Luo et al. (2012). Although previous studies with UVic have given rates of N₂ fixation between 128 and 150 Tg N yr⁻¹ (Landolfi et al., 2017; Keller et al., 2012), the CTR simulation in our configuration estimates global N₂ fixation rates of 219 Tg N yr⁻¹. In our case, this is due to the additional integration of benthic denitrification, which has not always been considered in previous UVic studies. To compensate for this additional N sink, the model estimates higher fixation rates.

210 Previous studies have shown that increasing atmospheric N deposition could lead to a reduction in N₂ fixation, due to non-nitrogen-fixing phytoplankton being more competitive than N fixers, when key nutrients like iron and phosphate are limiting (Jickells et al., 2017; Somes et al., 2016; Krishnamurthy et al., 2009, 2007). Reductions in N₂ fixation can partly explain the lower NO₃ concentrations at the surface of the tropical and subtropical oceans in NEWS, in areas that are far from riverine N input. Figure 8 shows that N₂ fixation is only slightly lower in the NEWS simulations than in CTR in the tropical and subtrop-
215 ical oceans, with some exceptions in the Pacific and the South Atlantic Ocean. However, N₂ fixation is reduced significantly in the regions, where NO₃ is also substantially lower, as seen before in the Bay of Bengal and near the Amazon River (Fig. 8 compared to Fig. 6).

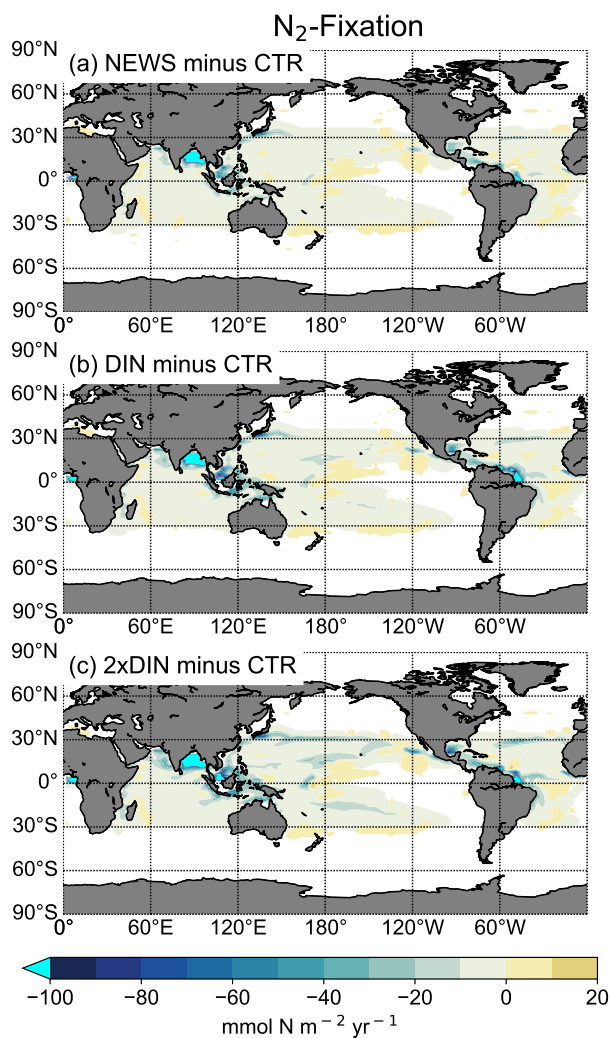


Figure 8. (a) Difference in annual vertically integrated rates of N_2 fixation calculated from UVic NEWS and CTR in $\text{mmol N m}^{-2} \text{s}^{-1}$. b. Difference in N_2 fixation in the simulation with riverine DIN and DON. c. Difference in N_2 fixation in the simulation with twice the amount of DIN. The white areas show regions where differences are smaller than $0.01 \text{ mmol N m}^{-2} \text{s}^{-1}$. Local minimas can be found near the Amazon river basin (from $-356 \text{ mmol N m}^{-2} \text{yr}^{-1}$ in NEWS-CTR to $-382 \text{ mmol N m}^{-2} \text{yr}^{-1}$ in DIN-CTR), in the Bay of Bengal (from $-347 \text{ mmol N m}^{-2} \text{yr}^{-1}$ to $-646 \text{ mmol N m}^{-2} \text{yr}^{-1}$ in 2xDIN-CTR) and in the Gulf of Guinea (from $-180 \text{ mmol N m}^{-2} \text{yr}^{-1}$ in NEWS-CTR to $-303 \text{ mmol N m}^{-2} \text{yr}^{-1}$ in 2xDIN-CTR).

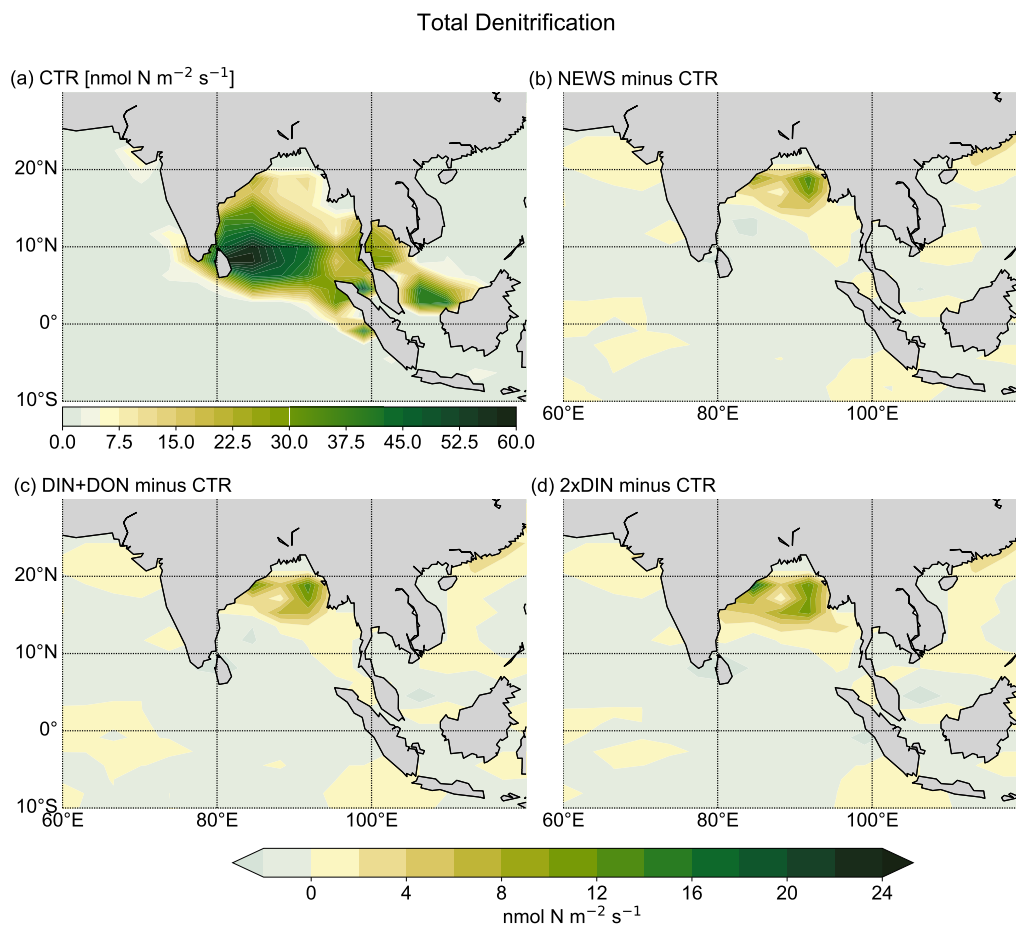


Figure 9. Total (water column and benthic) denitrification in the Bay of Bengal (a) Total denitrification from CTR in $\text{nmol N m}^{-2} \text{s}^{-1}$. (b) Difference in denitrification between NEWS and CTR. (c) Difference in denitrification between DIN+DON and CTR. (d) Difference in denitrification between 2xDIN and CTR.

Landolfi et al. (2013) found that the negative feedback mechanism between N_2 fixation and denitrification, generally stabilizing the marine N inventory, can turn into a destabilizing positive feedback, generating runaway N loss, if a close spatial association of N_2 fixation and denitrification occurs. This is due to the stoichiometry of denitrification, which consumes ~ 7 mol NO_3 for every mole of organic N if remineralized anaerobically in regions with low oxygen concentrations. In the Bay of Bengal, oxygen concentrations even though higher at the surface in NEWS than in CTR, are very low in the NEWS simulations in the subsurface waters and the whole deeper basin (Fig. 7). These suboxic waters are furthermore located in proximity to riverine N input and high denitrification rates (Fig. 9). While total denitrification rates (benthic and water column denitrification) are already quite high in CTR, they are further increased in NEWS, DIN+DON and 2xDIN in the northern Bay of Bengal, adjacent to the river delta.

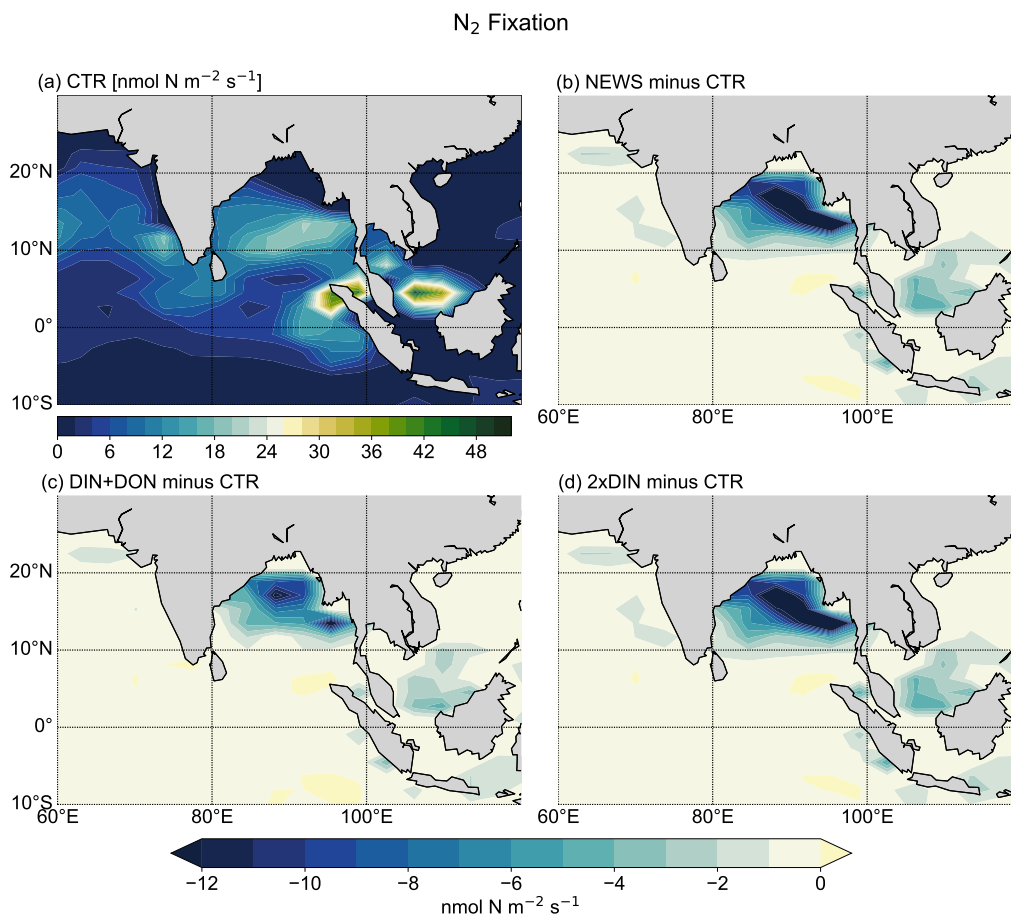


Figure 10. N₂ fixation in the Bay of Bengal (a) N₂ fixation from CTR in nmol N m⁻² s⁻¹. (b) Difference in N₂ fixation between NEWS and CTR. (c) Difference in N₂ fixation between DIN+DON and CTR. (d) Difference in N₂ fixation between 2xDIN and CTR

The 'vicious cycle' described by Landolfi et al. (2013) is triggered here by the input of new N from riverine export near oxygen minimum zones, explaining the NO₃ deficit found in the simulated Bay of Bengal (Fig. 5). Note that UVic, similar to most other biogeochemical ocean models, misplaces the main oxygen minimum zone from the Arabian Sea to the Gulf of Bengal (Séférián et al., 2020). In reality, high water column denitrification has been observed in the Arabian Sea, while in the Gulf of Bengal highly variable oxygen concentrations seem to inhibit denitrification (Johnson et al., 2019; Bange et al., 2005).

At the end of the simulation, the global marine N inventory is higher by 5278 Tg N in NEWS compared to CTR, which corresponds to 1.12 % of the global N inventory in CTR and 2.3 % of the total riverine N input over the 10000 years of the simulation. Even for the highest scenario (2xDIN), the total increase in global N represents only +2.53 % of the reference N inventory. Most of the additional N input through river discharge is thus compensated for by the feedbacks of the N cycle.



Table 3. Global nitrogen sources (river supply, N₂ fixation) and sinks (denitrification) averaged over the last 100 years of the simulations. All fluxes are given in Tg N yr⁻¹.

Simulation	River supply	N ₂ fixation	Water column denitrification	Benthic denitrification
UVic CTR	0.0	219.1	110.9	108.7
UVic NEWS	22.8	205.9	113.2	115.9
UVic DIN+DON	34.6	199.3	114.7	119.7
UVic 2xDIN	45.6	192.7	116.1	122.7

However, relative to the total additional input, the N increase in 2xDIN is higher than in NEWS (+2.6 % compared to +2.3 %), which means that the negative feedbacks do not compensate in 2xDIN as much as in NEWS. A possible reason for this result could be, that the main negative feedbacks, resulting in loss of N, take place in very localized low-oxygen areas, that can not expand further (e.g. Bay of Bengal, Amazon river mouth), while riverine N is supplied through river mouths scattered over the world.

3.2 Marine primary production

The rates of simulated annual global net primary production (NPP) compare well to present day estimates of annual global NPP (51 to 67 Pg C yr⁻¹) derived from satellite measurements (Buitenhuis et al., 2013; Westberry et al., 2008; Carr et al., 2006; Behrenfeld et al., 2005) and vary only little between the simulations. That is NPP increases only slightly with riverine N supply.

Annual averaged and vertically integrated primary production rates from CTR shows high rates in the equatorial eastern Pacific, Atlantic and Indian Ocean as well as in the upwelling region of the western south Atlantic Ocean (Fig. 11, a.). This global pattern persists in the simulations with riverine N supply (differences are small in Fig. 11, b.-d.). Nevertheless, with rivers supplying N to the ocean, differences are visible at smaller scale: NPP increases locally, close to the river mouths, especially near the coasts of Europe, China, parts of North and parts of South America. Most changes range between -60 and +100 g C m⁻² yr⁻¹. In isolated regions, marine primary production rates are lower in the three NEWS simulations than in CTR. This is particularly striking in parts of the Bay of Bengal, but also in the equatorial west Atlantic Ocean, to the north of the Amazon river mouth. In large regions of the subtropical and tropical oceans where surface NO₃ concentrations in our simulations are lower than in CTR, NPP differences also show a decrease.

In NEWS, where only DIN is supplied by the rivers, NPP increases mainly in shelf and near coastal oceans. However, higher amounts of N added by the rivers in DIN+DON and 2xDIN also impact marine productivity in the open ocean, far away from the river mouths. In the western subtropical and tropical waters NPP decreases with higher N input. In the higher northern



NPP

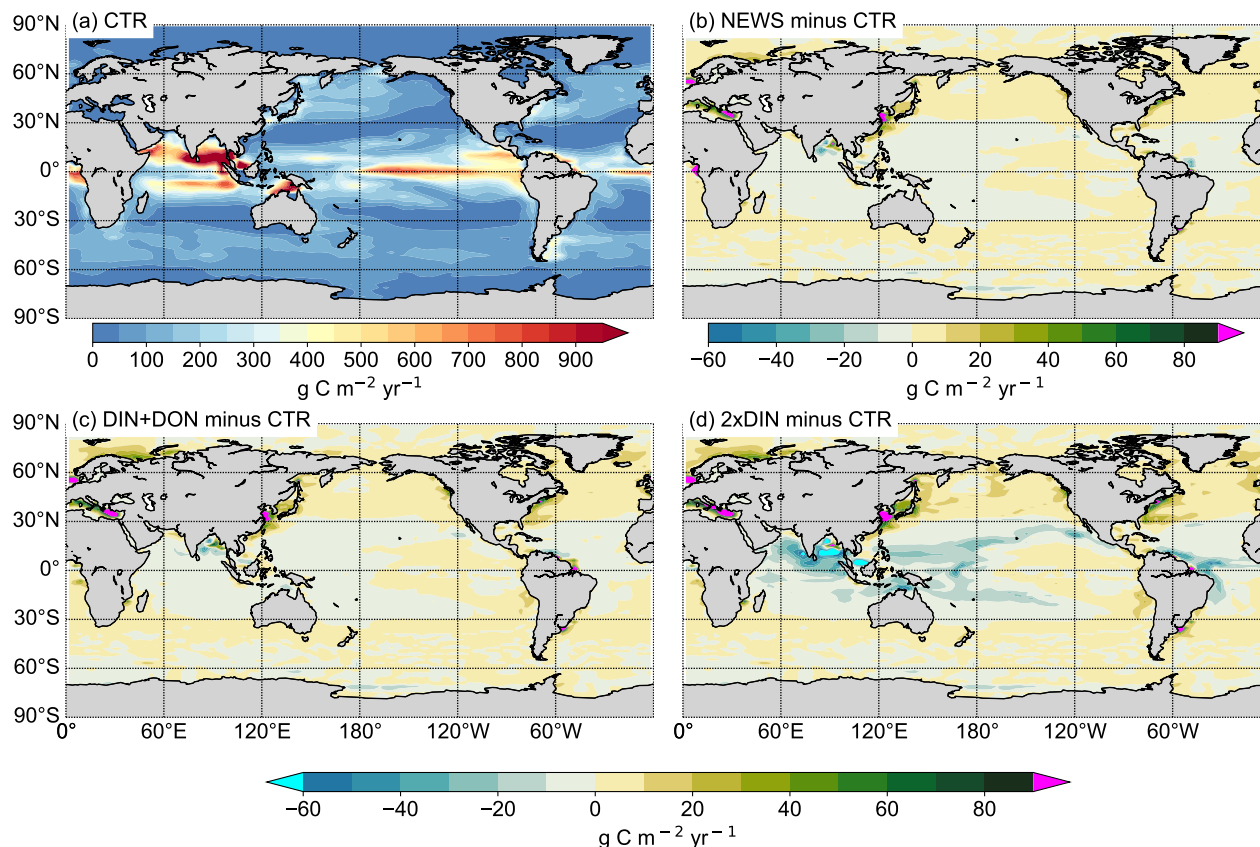


Figure 11. (a) Annual vertically integrated rates of primary production (NPP) calculated from UVic CTR in $\text{g C m}^{-2} \text{yr}^{-1}$. (b)-(d) Differences in NPP distribution calculated from different UVic simulations with riverine N export and from UVic simulation without riverine nutrient input (CTR) in $\text{g C m}^{-2} \text{yr}^{-1}$. (b) NPP from NEWS with with riverine DIN. (c) NPP in the simulation with riverine DIN and DON. (d) NPP in the simulation with twice the amount of DIN. The extreme values shown in cyan and red in these panels are listed in Table 5.

260 latitudes primary production is enhanced off the coastal oceans, in the North Atlantic and the western North Pacific Oceans
 as well as on the Arctic Ocean shelf (Fig. 11d.). Two "physical" explanations suggest themselves: first, near the coast the
 riverine N is consumed until phosphate becomes limiting. Then, the excess N is exported from the coastal oceans, leading to
 higher productivity farther away. Second, decreasing NPP in the open ocean can be the consequence of a seesaw effect, also
 called "nutrient robbing". Because higher N concentrations increase NPP in the coastal ocean, other nutrients, like P, are also
 265 consumed here instead of being exported to the open ocean. This can lead to lower rates of primary production farther away
 (Giraud et al., 2008).

Globally the differences in NPP in NEWS compared to the control simulation are close to the spatial variance of annually



Table 4. Mean annual depth-integrated NPP from model data and observations

Source	NPP [Pg C yr ⁻¹]	Description
UVic CTR	54.9	Model
UVic NEWS	55.3	Model
UVic DIN+DON	55.5	Model
UVic 2xDIN	55.7	Model
Behrenfeld et al. (2005)	67	Satellite data
Carr et al. (2006)	51	Mean of 31 global models
Westberry et al. (2008)	52	Carbon based, spectral
Buitenhuis et al. (2013)	56	Model and observational database

averaged NPP in the model ($\sim 57 \text{ g C m}^{-2} \text{ yr}^{-1}$). Most changes are smaller than $\pm 40 \text{ g C m}^{-2} \text{ yr}^{-1}$ ($\pm 2 \%$), even though locally the changes can be high (down to $-122 \text{ g C m}^{-2} \text{ yr}^{-1}$ in the Bay of Bengal, or even higher than $+500 \text{ g C m}^{-2} \text{ yr}^{-1}$ in the East China Sea). The total increase in NPP varies between $+0.7 \%$ (NEWS) and $+1.3 \%$ (2xDIN) compared to CTR. These changes reflect in wide parts changes in NO_3 due to the riverine inputs, except for the higher latitudes and other regions, where light-, temperature- or iron-limitation occur. In the higher DIN experiment, NPP is globally a little higher than in the other simulations including CTR, but the distribution shows NPP hot-spots near the river mouths, which are compensated by losses in the subtropical and tropical oceans.

As stated before, decreasing N_2 fixation together with higher rates of denitrification partly compensate for the additional N from riverine export and by this buffer the increase in NPP. Note in this regard that a small fraction of NPP is primary production by diazotrophs, which is lower in the NEWS simulations than in CTR ($-0.09 \text{ Pg C yr}^{-1}$ for NEWS, not shown here). The increase in NPP is mainly driven by higher rates near the river mouths whereas primary production declines in regions, where rates of N_2 fixation are lower as a reaction to the input of riverine N, like in the Gulf of Bengal and near the Amazon river mouth, but also in parts of the open subtropical and tropical oceans (Fig. 8, Fig. 10 and Fig. 11). This shows also, that the response of ocean biogeochemistry depends on the region where riverine DIN first reaches the ocean. One can therefore ask the question, which rivers have the highest influence on global marine biogeochemistry?

3.3 Simulations with regionally activated riverine nitrogen supply

To answer this question, we performed five additional experiments with the same configuration as in the NEWS simulation before, but this time only the rivers of one of five parts of the world transport NO_3 to the ocean. The five scenarios simulate the nutrient supply from North American rivers (NAM), South American rivers (SAM), European and Russian rivers (EUR), Asian rivers (ASIA) and African rivers (AFR), respectively.



Table 5. Minimum and maximum values of NPP difference to CTR simulation as shown in Figure 11

Region	Difference in NPP [$\text{g C m}^{-2} \text{ yr}^{-1}$]
UVic NEWS	
Bay of Bengal	-62
Yellow Sea	502
North Sea	246
Rio de la Plata river mouth	182
Eastern Mediterranean Sea	114
UVic DIN	
Bay of Bengal	-69
Yellow Sea	501
North Sea	274
Rio de la Plata river mouth	258
Eastern Mediterranean Sea	124
UVic 2xDIN	
Bay of Bengal	-122
Yellow Sea	544
North Sea	337
Rio de la Plata river mouth	261
Eastern Mediterranean Sea	130

Total riverine N input varies depending on the rivers. Therefore, the amount of N added to the ocean is different in each of the five scenarios. The highest amount of N is added by Asian rivers ($11.7 \text{ Tg N yr}^{-1}$). Rivers from South America export 3.5 Tg N yr^{-1} , followed by rivers in EUR (3.2 Tg N yr^{-1}). The lowest input scenarios are NAM (2.6 Tg N yr^{-1}) and AFR (2.3 Tg N yr^{-1}). The three ocean basins are then affected differently depending on the scenario.

Compared to the control simulation (Fig. 12), the differences in NO_3 concentrations are small ($0\text{-}2 \text{ mmol / m}^3$), but the patterns differ depending on the origin of NO_3 . It appears that all ocean basins are most affected by rivers in Europe and Russia (EUR) and least affected by rivers from South America (SAM), although rivers from this region provide the second highest N supply to the global oceans. The Atlantic Ocean is most affected by rivers in EUR and to a lesser extent from NAM. Asian rivers lead to a local increase of NO_3 concentrations in the Northern Pacific in the upper 2000 m. Here, NO_3 is trapped because North Pacific waters upwell in the North Pacific. Extra nitrogen is used by local biota and exported again within the North Pacific. But globally and over all depths, rivers in EUR and to a lesser extent in NAM have the biggest impact on NO_3 concentrations in the Pacific. Rivers in SAM slightly decrease NO_3 concentrations in large parts of the Pacific Ocean.

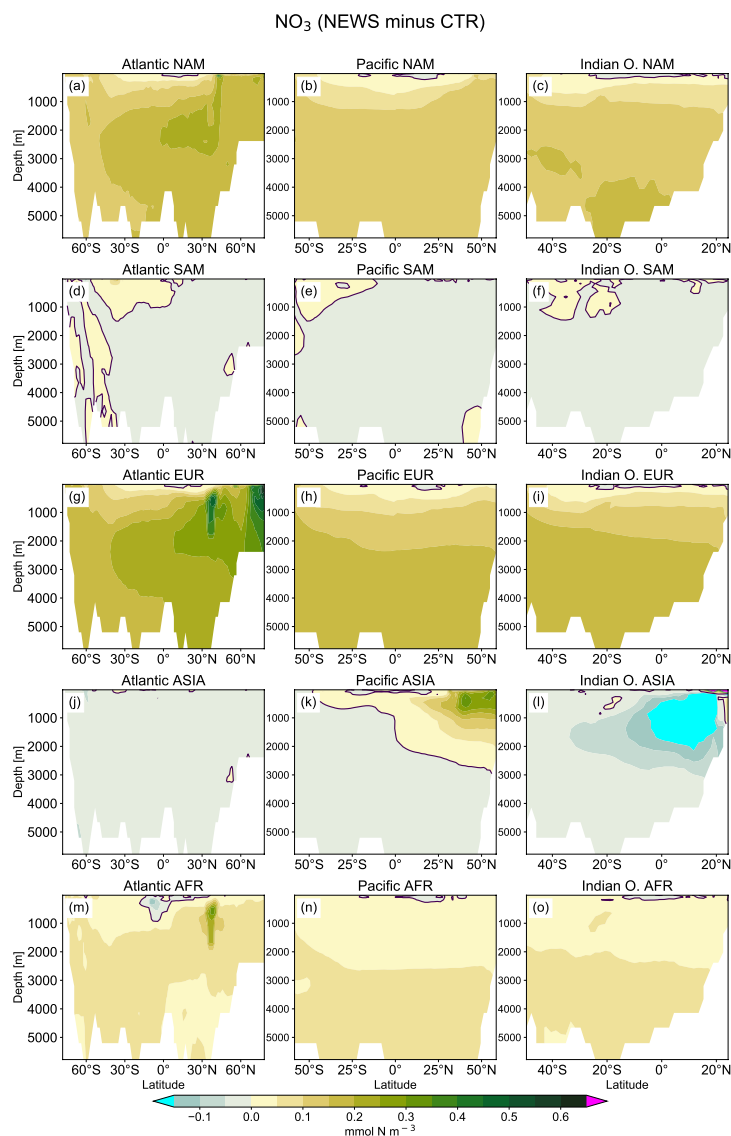


Figure 12. Difference of the zonal mean concentrations of NO_3 in the main ocean basins (Atlantic, Pacific and Indian Ocean) between regional NEWS and the control simulation (CTR). The regional simulations show export from rivers in North America (a-c), South America (d-f), Europe and Russia (g-i), Asia (j-l) and Africa (m-o), respectively. The violet line indicates the 0.0 mmol N m^{-3} contour line. Note in the Indian Ocean ASIA the cyan and magenta colored grid points, indicating lower (minimum at $-0.9 \text{ mmol N m}^{-3}$) and higher values (maximum at $2.5 \text{ mmol N m}^{-3}$) than the colorbar.

300 In the Indian Ocean basin, NO_3 concentrations are higher in the simulations NAM, EUR and AFR. This is because global circulation transports N to remote ocean basins. In contrast, zonally averaged NO_3 concentrations are lower in the northern



Table 6. Global NPP from different UVic simulations

Simulation	NPP in Pg C yr ⁻¹
UVic NEWS	55.34
UVic CTR	54.94
AFR	54.99
ASIA	55.04
EUR	55.08
NAM	54.99
SAM	54.96

Indian Ocean, if Asian rivers supply N and thereby enhance denitrification (Fig. 12). N from other regions does not trigger the 'vicious cycle' (Landolfi et al., 2013) in the Bay of Bengal, in the model, because it arrives and is used in biological production in other regions, before it can reach the Bay of Bengal.

305 In all simulations with regionally activated riverine nutrient input, N₂ fixation rates are lower than in CTR, with differences ranging between -0.8 Tg N yr⁻¹ in EUR to -7.7 Tg N yr⁻¹ in ASIA (not shown here). This decrease is most prominent in the Bay of Bengal for experiment ASIA, because high DIN export from the Ganges Delta gives the advantage to non-N-fixing phytoplankton, which outcompete diazotrophs.

Generally, rivers that enter well-oxygenated eutrophic oceans with little N₂ fixation have largest impact on the global ocean N
310 inventory. This is especially the case for rivers from EUR and NAM, entering the Atlantic and Arctic oceans at higher northern latitudes. In contrast, the Amazon in SAM is located in an oxygen-deficient region in the tropical Atlantic. The main riverine N supply in ASIA increases N concentrations in the higher northern latitudes of the Pacific, but leads to a net loss of N in the Bay of Bengal.

This has consequences for marine productivity: although NPP is higher in NEWS in most of the coastal oceans, where rivers
315 export DIN, NPP is considerably lower in three regions, where the positive vicious-cycle feedbacks dominate: in AFR in the Gulf of Guinea, in ASIA in the Gulf of Bengal and in SAM, where the river plume of the Amazon river enters the tropical Atlantic Ocean (Fig. 13).

The global NPP rates range from 54.96 Pg C yr⁻¹ in SAM to 55.08 Pg C yr⁻¹ in the EUR simulation (Table 6). EUR contributes
320 most to a widespread increase in NPP due to riverine NO₃, while ASIA only increases NPP in parts of the ocean and decreases primary production in others.

The regional simulations have shown, that the ecosystem's response to riverine N supply differs depending on the region of the supply and does not always result in an increase of marine NPP. Note that the sum of the NPP changes in the regional experiments is equal to the change in NEWS, except for parts of the Southern Ocean and the eastern Mediterranean Sea. In

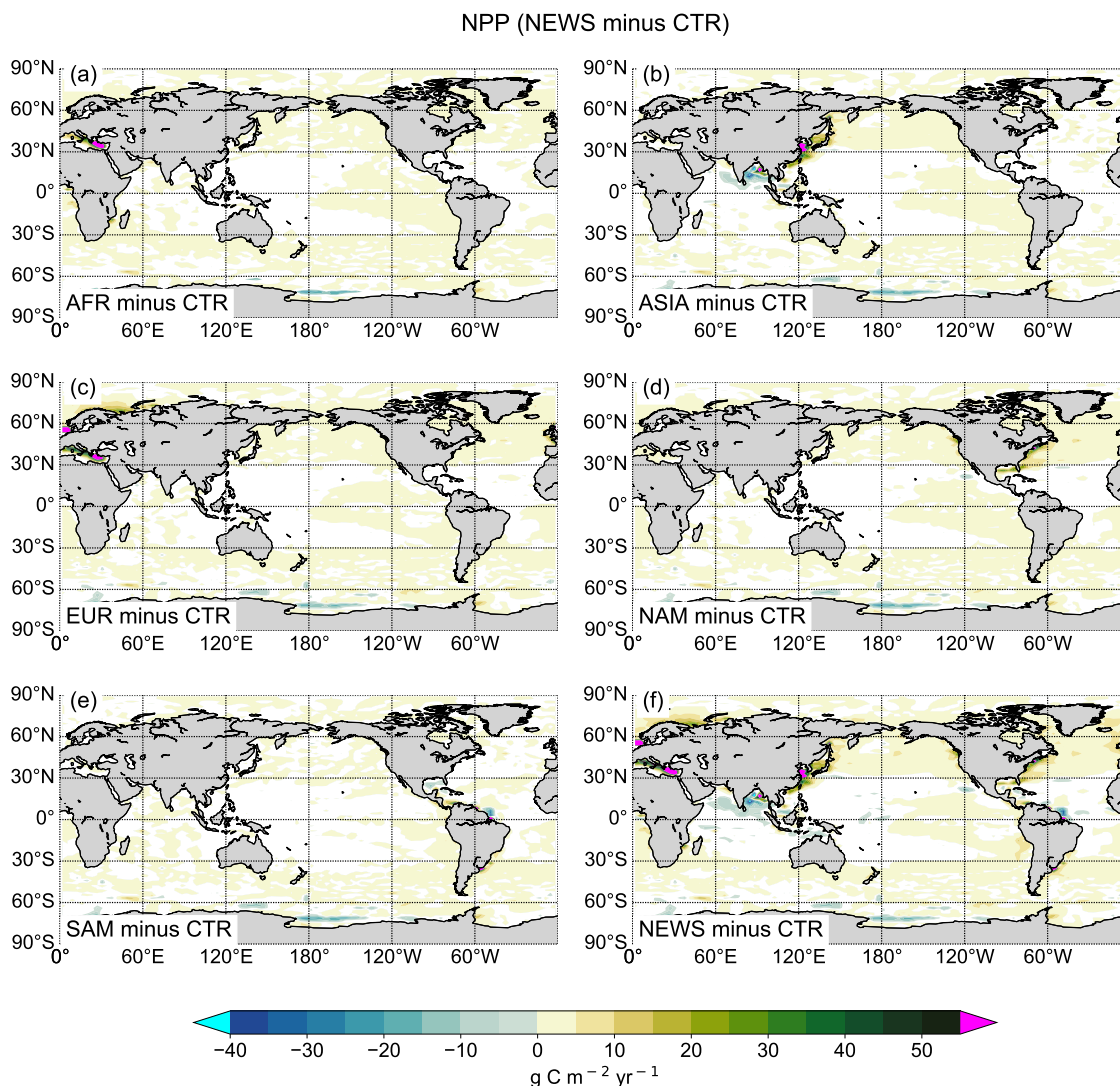


Figure 13. Difference of the global vertically integrated rates of primary production (NPP) between regional NEWS and the control simulation (CTR). The regional simulations show export from rivers in Africa (a), Asia (b), Europe and Russia (c), North America (d) and South America (e). The cyan and magenta colored regions mark grid points with values outside the colorbar range, similar to the values in Figure 11. In the white regions differences between the simulations are very small, between -10 and $+10$ g C m⁻² yr⁻¹.

the Mediterranean Sea, the sum of the regional NPP changes compared to CTR is higher by 1,8 % than the change in global NEWS. This is due to phosphate limitation in this region in the model, inhibiting additional NPP in the NEWS simulation.



4 Limitations and further discussion

The results of the simulations with UVic and riverine N have to be evaluated in the context of previous studies. Lacroix et al. (2020) for example found that adding riverine nutrient supply increased primary production essentially in some "hot-spots" near the river mouths. While we have observed a qualitatively similar phenomenon in our simulations, these hot-spots differ
330 between both studies. This is due partly to the coarser resolution of UVic. From the semi-enclosed seas, which present higher NPP in the study by Lacroix et al. (2020), only the Yellow Sea is adequately resolved in UVic and shows also a significant increase in NPP. But the patterns of primary production differ in several other aspects. Where NPP is highly increased in the subtropical and tropical eastern Pacific in Lacroix et al. (2020), there is hardly any change in UVic-NEWS. In the Bay of Bengal, where we found decreased NPP upon addition of riverine N supply in UVic, their model simulates an increase.
335 The main reason for these differences is the fact, that Lacroix et al. (2020) included more than just N from river discharge. Especially the supply in additional phosphate plays an important role for NPP, and is for example particularly high in the Bay of Bengal in their simulation. Furthermore, the magnitudes of oceanic nutrient inputs do not differ substantially between the two simulations analyzed in the study of Lacroix et al. (2020): the total N input is 25.2 Tg N yr⁻¹ for the reference simulation (REF) and 27.0 Tg N yr⁻¹ for the simulation with riverine nutrient supply (RIV). The reference distributions of NPP (REF) in
340 Lacroix et al. (2020) also differs with regard to UVic. NPP from UVic is notably higher in the Indian Ocean and the western tropical Atlantic, but lower in the Southern Ocean. These absolute higher values of NPP in the open oceans can be accounted for by the parameterisation of NPP in our model, where open oceans have to compensate for the lack of higher coastal production in order to achieve estimated annual NPP within the range of 51 to 67 Pg C yr⁻¹, that include coastal NPP (Keller et al., 2012). But as both reference distributions of NPP differ (from Lacroix et al. (2020) and CTR), it is no surprise, that NPP also presents
345 different patterns in the simulations with riverine nutrient supply (RIF and NEWS, respectively). Riverine nutrients only reach the ocean in very localized areas. In our simulation with the NEWS data set from Mayorga et al. (2010), we overestimate the effects of adding N from river discharge, because DIN is exported directly from the river mouth to the ocean, as our global model does not fully resolve shelf seas and coastal oceans. In reality, part of these nutrients stays on the shelf or is buried or denitrified in coastal sediments. We also do not account for the buffer effect of the coasts, that could
350 be parameterised, as shown by Sharples et al. (2017) and Izett and Fennel (2018). Nevertheless, even without taking these trapping processes into account, the biogeochemical feedbacks of the ocean buffer higher increases in N concentrations. The absolute increase in marine primary production is small (between +0.7 % in NEWS and +1.3 % in 2xDIN). However, other studies with additional N supply also found only moderate increase in primary production rates. Da Cunha et al. (2007) for example predicts increases in NPP up to +5 % for the global ocean, but using a high DIN scenario which
355 includes 7.1 Tmol N yr⁻¹ (corresponding to ~ 100 Tg N yr⁻¹). Da Cunha et al. (2007) also include silicate, iron and dissolved inorganic carbon, but concluded that riverine N may have the higher impact on primary production. Like Somes et al. (2016), who also simulated a very small increase in NPP upon the addition of N deposition in their model, we found that decreasing N₂ fixation and increasing denitrification act globally as negative feedbacks and partly compensate for the riverine N supply. In regions of low oxygen concentrations, these feedbacks even overcompensate the external perturbation



360 in terms of riverine N supply, by forming a "vicious cycle" (Landolfi et al., 2013), consuming more N than provided by the rivers. This is especially the case in the Bay of Bengal. However, we are aware of the fact that UVic, like several other models, currently misplaces the oxygen minimum zone from the Arabian Sea to the Bay of Bengal. It is likely, that N supply by Asian rivers would lead to a somewhat larger increase in the oceanic N inventory, if the high nutrient input from the Ganges Delta would not meet the high denitrification zone in the Indian Ocean (Johnson et al., 2019).

365 Including other nutrients in addition to N, especially P, could change the setting, especially in regions that are phosphate limited. While this is the logical continuation of the current study, the scope of this project was to explore the consequences of locally high N injections on the N cycle and its feedbacks. Furthermore, as rivers supply relatively more N than P to the global ocean, excess N would still be supplied to the coastal oceans (Turner et al., 2003).

5 Conclusion

370 In this study a new model component was added to the global Earth System Model UVic, simulating DIN supply from river discharge. At the end of the 10000 years of simulations, the N budget has reached a new steady state. We have shown, that riverine N added to the coastal ocean is taken up by near-coastal biology but also exported in the deeper ocean and circulated worldwide. Despite the continuous addition of N to the system, global marine N concentrations and marine productivity are not increased substantially (+ 1.12 % N and + 0.72 % for NPP) in our simulations. The globally negative feedbacks of the N

375 cycle buffer most of the increase in NO₃ concentrations and NPP. N₂ fixation decreases promptly after the beginning of the simulations, partly compensating for the additional N at the surface of the ocean, likewise to the N deposition experiments by Somes et al. (2016) and Landolfi et al. (2017). Water column and benthic denitrification are higher compared to a control simulation without riverine N input and play an important role in low-oxygen regions that, moreover tend to expand upon the addition of riverine N supply and generate a net N loss.

380 The additional N input triggers only a small NPP increase and mostly in proximity to the river mouths. In our regional simulations we have shown, that NPP can even decrease locally depending on the region where N reaches the ocean. While N from river discharges from North America and Europe (and Russia) is also circulated and exported to the deeper ocean, N from Asian rivers is trapped in the western Pacific or even partly lost via denitrification in oxygen-deficient regions, like it is the case in the modeled Bay of Bengal.

385 We have seen that the biogeochemical feedbacks of the ocean buffer higher increases in N concentrations and NPP. Hence, the result suggests also, that ocean fertilization with nitrogen alone (as proposed for example by Harrison (2017)) may not have the desired effect. Indeed, simulated carbon export increases globally by only 0.06 Pg C yr⁻¹ in our NEWS simulation, representing less than 10 % of the amount estimated by Harrison (2017) to be the upper limit of sequestered carbon in the ocean from on-going fertilization with nitrogen.

390 Our study emphasizes the importance of understanding the feedbacks of the marine biogeochemistry in general and the N cycle in particular in order to predict the response of the system to changes in riverine nutrient supply. We have found, that river discharge as part of the coastal system is relevant for the marine biology not only locally, but also for the global ocean.



395 But while atmospheric deposition provides only N, rivers supply also P to the ocean. Adding P in addition to N in the coastal oceans may change the response of the ecosystem, especially if N limitation is overcome. Tyrrell (1999) stated, that nitrate is the "proximate limiting" nutrient in surface waters, the most limiting nutrient to instantaneous growth. Including phosphate, as the "ultimately limiting nutrient", could change our story on longer time scales. Future research will therefore include model experiments with the combination of riverine nitrogen and phosphorus.

400 *Code and data availability.* The model code we used as well as input and output data are available online (Tivig, Miriam, Keller, David P., and Oschlies, Andreas (2020). Supplementary Data to "Feedbacks in the marine nitrogen cycle limit the impact of riverine nitrogen supply on global marine biology and biogeochemistry in an Earth System Model ", [hdl:20.500.12085/59977a36-e8e7-4348-a4e8-2b13f3913590](https://hdl.handle.net/20.500.12085/59977a36-e8e7-4348-a4e8-2b13f3913590)). More information on the original NEWS2 data set is available from the Global NEWS group at the web site http://icr.ioc-unesco.org/index.php?option=com_content&view=article&id=45&Itemid=100002. Please email Emilio Mayorga at mayorga@marine.rutgers.edu to obtain this data set.

405 *Author contributions.* MT developed the research concept in discussion with AO and DPK. DPK provided the initial model code, which was further developed, run, and analysed by MT. MT analysed the model output and visualised the results. MT wrote the manuscript with contributions from all co-authors.

Competing interests. The authors declare that they have no conflict of interest.

410 *Acknowledgements.* We gratefully acknowledge E. Mayorga, S. Seitzinger and their co-authors for making their database of Global Nutrient Export from WaterSheds 2 (NEWS2) available for our study. AO and DPK acknowledge funding from the European Union's Horizon 2020 Research and Innovation Program under grant 820989 (project COMFORT, "Our common future ocean in the Earth system — quantifying coupled cycles of carbon, oxygen, and nutrients for determining and achieving safe operating spaces with respect to tipping points") and OceanNETs (grant #869357). This work was also supported by the German Research Foundation (DFG) as part of the research project SFB 754 "Climate-Biogeochemistry Interactions in the Tropical Ocean". We would also thank the GEOMAR's Biogeochemical Modelling group for many fruitful discussions.



415 References

- Altabet, M. A.: Constraints on oceanic N balance/imbalance from sedimentary ^{15}N records, *Biogeosciences*, 4, 75–86, <https://doi.org/10.5194/bg-4-75-2007>, 2006.
- Bange, H., Naqvi, S., and Codispoti, L.: The nitrogen cycle in the Arabian Sea, *Progress in Oceanography*, 65(2-4), 145–158, <https://doi.org/10.1016/j.pocean.2005.03.002>, 2005.
- 420 Barron, C. and Duarte, C. M.: Dissolved organic carbon pools and export from the coastal ocean, *Global Biogeochemical Cycles*, 29, 1725–1738, <https://doi.org/10.1002/2014GB005056>, 2015.
- Bauer, J. E., Cai, W. J., Raymond, P. A., Bianchi, T. S., Hopkinson, C. S., and Regnier, P. A. G.: The changing carbon cycle of the coastal ocean, *Nature*, 504, 61–70, <https://doi.org/10.1038/nature12857>, 2013.
- Behrenfeld, M. J., Boss, E., Siegel, D. A., and Shea, D. M.: Carbon-based ocean productivity and phytoplankton physiology from space, 425 *Global Biogeochemical Cycles*, 19, GB1006, <https://doi.org/10.1029/2004GB002299>, 2005.
- Bernard, C. Y., Dürr, H. H., Heinze, C., Segschneider, J., and Maier-Reimer, E.: Contribution of riverine nutrients to the silicon biogeochemistry of the global ocean – a model study, *Global Biogeochemical Cycles*, 8, 551–564, <https://doi.org/10.5194/bg-8-551-2011>, 2011.
- Beusen, A. H. W., Bouwman, A. F., Beek, L. P. H. V., Mogollon, J. M., and Middelburg, J. J.: Global riverine N and P transport to ocean increased during the 20th century despite increased retention along the aquatic continuum, *Biogeosciences*, 13, 2441–2451, 430 <https://doi.org/10.5194/bg-13-2441-2016>, 2016.
- Billen, G. and Garnier, J.: River basin nutrient delivery to the coastal sea: Assessing its potential to sustain new production of non-siliceous algae, *Marine Chemistry*, 106, 148–160, <https://doi.org/10.1016/j.marchem.2006.12.017>, 2007.
- Bohlen, L., Dale, A. W., and Wallmann, K.: Simple transfer functions for calculating benthic fixed nitrogen losses and C:N:P regeneration ratios in global biogeochemical models, *Global Biogeochemical Cycles*, 26, GB3029, <https://doi.org/10.1029/2011GB004198>, 2012.
- 435 Buitenhuis, E. T., Hashioka, T., and Quéré, C. L.: Combined constraints on global ocean primary production using observations and models, *Global Biogeochemical Cycles*, 27, 847–858, <https://doi.org/10.1002/gbc.20074>, 2013.
- Capone, D. G., Zehr, J. P., Paerl, H. W., Bergmann, B., and Carpenter, E. J.: *Trichodesmium*, a globally significant marine cyanobacterium, *Science*, 276, 1221–1229, 1997.
- Carr, M.-E., Friedrichs, M. A. M., Schmeltz, M., Aita, M. N., Antoine, D., Arrigo, K. R., Asanuma, I., Aumont, O., Barber, R., Behrenfeld, M., Bidigare, R., Buitenhuis, E. T., Campbell, J., Ciotti, A., Dierssen, H., Dowell, M., Dunne, J., Esaias, W., Gentili, B., Gregg, 440 W., Groom, S., Hoepffner, N., Ishizaka, J., Kameda, T., Quéré, C. L., Lohrenz, S., Marra, J., Mélin, F., Moore, K., Morel, A., Reddy, T. E., Ryan, J., Scardi, M., Smyth, T., Turpie, K., Tilstone, G., Waters, K., and Yamanaka, Y.: A comparison of global estimates of marine primary production from ocean color, *Deep Sea Research Part II: Topical Studies in Oceanography*, 53, 741–770, <https://doi.org/10.1016/j.dsr2.2006.01.028>, 2006.
- 445 Claussen, M., Mysak, L. A., Weaver, A. J., Crucifix, M., Fichet, T., Loutre, M.-F., Weber, S., Alcamo, J., Alexeev, V., Berger, A., Calov, R., Ganopolski, A., Goosse, H., Lohmann, G., Lunkeit, F., Mokhov, I., Petoukhov, V., Stone, P., and Wang, Z.: Earth System Models of Intermediate Complexity: Closing the Gap in the Spectrum of Climate System Models, *Climate Dynamics*, 18, 579–586, <https://doi.org/10.1007/s00382-001-0200-1>, 2002.
- Codispoti, L. A.: Is the ocean losing nitrate?, *Nature*, 376, 1995.
- 450 Codispoti, L. A., Brandes, J. A., Christensen, J. P., Devol, A. H., Naqvi, S. A., Paerl, H. W., and Yoshinari, T.: The oceanic fixed nitrogen and nitrous oxide budgets: Moving targets as we enter the anthropocene?, *Scientia Marina*, 65, 85–105, 2001.



- Da Cunha, L., Buitenhuis, E., Le Quéré, C., Giraud, X., and Ludwig, W.: Potential impact of changes in river nutrient supply on global ocean biogeochemistry, *Global Biogeochemical Cycles*, 521, GB4007, <https://doi.org/10.1029/2006GB002718>, 2007.
- DeMaster, D. J. and Pope, R. H.: Nutrient dynamics in Amazon shelf waters: results from AMASSEDS, *Continental Shelf Research*, 16 No. 03, 263–289, 1996.
- 455
- Deutsch, C., Gruber, N., Key, R. M., and Sarmiento, J. L.: Denitrification and N₂ fixation in the Pacific Ocean, *Global Biogeochemical Cycles*, 15, 483–506, 2001.
- Deutsch, C., Sarmiento, J. L., Sigman, D. M., Gruber, N., and Dunne, J. P.: Spatial coupling of nitrogen inputs and losses in the ocean, *Nature*, 445, 163–167, 2007.
- 460
- Dumont, E., Harrison, J. A., Kroeze, C., Bakker, E. J., and Seitzinger, S. P.: Impacts of Atmospheric Anthropogenic Nitrogen on the Open Ocean, *Global Biogeochemical Cycles*, 19, GB4S02, <https://doi.org/10.1029/2005GB002488>, 2005.
- Eby, M., Zickfeld, K., Montenegro, A., Archer, D., Meissner, K. J., and Weaver, A. J.: Lifetime of Anthropogenic Climate Change: Millennial Time Scales of Potential CO₂ and Surface Temperature Perturbations, *Journal of Climate*, 22, 2501–2511, <https://doi.org/10.1175/2008JCLI2554.1>, 2009.
- 465
- Eisele, A. and Kerimoglu, O.: MOSSCO River data basis – Riverine Nutrient inputs, Tech. rep., Helmholtz-Zentrum Geesthacht, https://www.hzg.de/imperia/md/images/hzg/institut_fuer_kuestenforschung/kosystemmodellierung/kosystemmodellierung/riverine_nutrient_inputs.pdf, 2015.
- Falkowski, P. G.: Evolution of the nitrogen cycle and its influence on the biological sequestration of CO₂ in the ocean, *Nature*, 387, 272–275, <https://doi.org/10.1038/387272a0>, 1997.
- 470
- Galloway, J. N., Dentener, F., Capone, D., Boyer, E., Howarth, R., Seitzinger, S., Asner, G., Cleveland, C., Green, P., Holland, E., Karl, D., Michaels, A., Porter, J., Townsend, A., and Vörösmarty, C.: Nitrogen cycles: past, present, and future, *Biogeochemistry*, 70, 153–226, <https://doi.org/10.1007/s10533-004-0370-0>, 2004.
- Garcia, H. E., Weathers, K., Paver, C. R., Smolyar, I., Boyer, T. P., Locarnini, R. A., Zweng, M. M., Mishonov, A. V., Baranova, O. K., Seidov, D., and Reagan, J. R.: Volume 4: Dissolved Inorganic Nutrients (phosphate, nitrate and nitrate+nitrite, silicate), in: *World Ocean Atlas 2018*, edited by Editor, A. M. T., p. 35pp, NOAA Atlas NESDIS 84, https://www.ncei.noaa.gov/data/oceans/woa/WOA18/DOC/woa18_vol4.pdf, 2019.
- 475
- Giraud, X., Quéré, C. L., and da Cunha, L. C.: Importance of coastal nutrient supply for global ocean biogeochemistry, *Global Biogeochemical Cycles*, 22, GB2025, <https://doi.org/10.1029/2006GB002717>, 2008.
- Gruber, N.: The Dynamics of the Marine Nitrogen Cycle and its Influence on Atmospheric CO₂ Variations, in: *The Ocean Carbon Cycle and Climate*, edited by Follows, M. and Oguz, T., pp. 97–148, Springer Netherlands, Dordrecht, https://doi.org/10.1007/978-1-4020-2087-2_4, 2004.
- 480
- Gruber, N. and Sarmiento, J. L.: Global patterns of marine nitrogen fixation and denitrification, *Global Biogeochemical Cycles*, 11, 235–266, <https://doi.org/10.1029/97GB00077>, 1997.
- Harrison, D. P.: Global negative emissions capacity of ocean macronutrient fertilization, *Environmental Research Letters*, 12, 035 001, <https://doi.org/10.1088/1748-9326/aa5ef5>, 2017.
- 485
- Holmes, R. M., McClelland, J. W., Peterson, B. J., Tank, S. E., Bulygina, E., Eglinton, T. I., Gordeev, V. V., Gurtovaya, T. Y., Raymond, P. A., Repeta, D. J., Staples, R., Striegl, R. G., Zhulidov, A. V., and Zimov, S. A.: Seasonal and Annual Fluxes of Nutrients and Organic Matter from Large Rivers to the Arctic Ocean and Surrounding Seas, *Estuaries and Coasts*, 35, 369–382, <https://doi.org/10.1007/s12237-011-9386-6>, 2012.



- 490 Izett, J. G. and Fennel, K.: Estimating the Cross-Shelf Export of Riverine Materials: Part 1. General Relationships From an Idealized Numerical Model, *Global Biogeochemical Cycles*, 32, 160–175, <https://doi.org/10.1002/2017GB005667>, 2018.
- Jahnke, R. A.: Global Synthesis, in: *Carbon and Nutrient Fluxes in Continental Margins*. Global Change – The IGBP Series, edited by Liu, K., Atkinson, L., Quiñones, R., and Talaue-McManus, L., Springer, Berlin, Heidelberg, <https://doi.org/10.1007/978-3-540-92735-8-16>, 2010.
- 495 Jickells, T. D., Buitenhuis, E., Altieri, K., Baker, A. R., Capone, D., Duce, R. A., Dentener, F., Fennel, K., Kanakidou, M., LaRoche, J., Lee, K., Liss, P., Middelburg, J. J., Moore, J. K., Okin, G., Oschlies, A., Sarin, M., Seitzinger, S., Sharples, J., Singh, A., Suntharalingam, P., Uematsu, M., and Zamora, L. M.: A reevaluation of the magnitude and impacts of anthropogenic atmospheric nitrogen inputs on the ocean, *Global Biogeochemical Cycles*, 31, 289–305, <https://doi.org/10.1002/2016GB005586>, 2017.
- Johnson, K. S., Riser, S. C., and Ravichandran, M.: Oxygen Variability Controls Denitrification in the Bay of Bengal Oxygen Minimum
500 Zone, *Geophysical Research Letters*, 46, 804–811, <https://doi.org/10.1029/2018GL079881>, 2019.
- Karl, D., Letelier, R., Tupas, L., Dore, J., Christian, J., and Hebel, D.: The role of nitrogen fixation in biogeochemical cycling in the subtropical North Pacific Ocean, *Nature*, 388, 533–539, 1997.
- Karl, D., Micalteas, A., Bergman, Capone, D., Carpenter, E., Letelier, R., Lipschultz, F., Paerl, H., Sigman, D., and Stal, L.: Dinitrogen fixation in the world's oceans, *Biogeochemistry*, 57/58, 47–98, 2002.
- 505 Keller, D. P., Oschlies, A., and Eby, M.: A new marine ecosystem model for the University of Victoria Earth System Climate Model, *Geoscientific Model Development*, 5, 1195–1220, <https://doi.org/10.5194/gmd-5-1195-2012>, 2012.
- Krishnamurthy, A., Moore, J. K., Zender, C. S., and Luo, C.: Effects of atmospheric inorganic nitrogen deposition on ocean biogeochemistry, *Journal of Geophysical Research*, 112, G02019, <https://doi.org/10.1029/2006JG000334>, 2007.
- Krishnamurthy, A., Moore, J. K., Mahowald, N., Luo, C., Doney, S. C., Lindsay, K., and Zender, C. S.: Impacts of increasing
510 anthropogenic soluble iron and nitrogen deposition on ocean biogeochemistry, *Global Biogeochemical Cycles*, 23, GB3016, <https://doi.org/10.1029/2008GB003440>, 2009.
- Lacroix, F., Ilyina, T., and Hartmann, J.: Oceanic CO₂ outgassing and biological production hotspots induced by pre-industrial river loads of nutrients and carbon in a global modeling approach, *Biogeosciences*, 17, 55–88, <https://doi.org/10.5194/bg-17-55-2020>, 2020.
- Landolfi, A., Dietze, H., Koeve, W., and Oschlies, A.: Overlooked runaway feedback in the marine nitrogen cycle: the vicious cycle, *Biogeosciences*, 10, 1351–1363, <https://doi.org/10.5194/bg-10-1351-2013>, 2013.
- Landolfi, A., Somes, C. J., Koeve, W., Zamora, L. M., and Oschlies, A.: Oceanic nitrogen cycling and N₂O flux perturbations in the Anthropocene, *Global Biogeochemical Cycles*, 31, 1236–1255, <https://doi.org/10.1002/2017GB005633>, 2017.
- Landolfi, A., Kähler, P., Koeve, W., and Oschlies, A.: Global Marine N₂ Fixation Estimates: From Observations to Models, *Frontiers in Microbiology*, 9, 2112, <https://doi.org/10.3389/fmicb.2018.02112>, 2018.
- 520 Lu, F.-H., Niab, H.-G., Liu, F., and Y.Zeng, E.: Occurrence of nutrients in riverine runoff of the Pearl River Delta, South China, *Journal of Hydrology*, 376 - Issues 1-2, 107–115, <https://doi.org/10.1016/j.jhydrol.2009.07.018>, 2009.
- Lu, X., Li, S., He, M., Zhou, Y., Bei, R., Li, L., and Ziegler, A. D.: Seasonal changes of nutrient fluxes in the Upper Changjiang basin: An example of the Longchuanjiang River, China, *Journal of Hydrology*, 205, 344–351, <https://doi.org/10.1016/j.jhydrol.2011.05.032>, 2011.
- Luo, Y.-W., Doney, S. C., Anderson, L. A., Benavides, M., Berman-Frank, I., Bode, A., Bonnet, S., Boström, K. H., Böttjer, D., Capone,
525 D. G., Carpenter, E. J., Chen, Y. L., Church, M. J., Dore, J. E., Falcón, L. I., Fernández, A., Foster, R. A., Furuya, K., Gómez, F., Gundersen, K., Hynes, A. M., Karl, D. M., Kitajima, S., Langlois, R. J., LaRoche, J., Letelier, R. M., Marañón, E., McGillicuddy Jr., D. J., Moisander, P. H., Moore, C. M., Mouriño Carballido, B., Mulholland, M. R., Needoba, J. A., Orcutt, K. M., Poulton, A. J., Rahav, E., Raimbault, P.,



- Rees, A. P., Riemann, L., Shiozaki, T., Subramaniam, A., Tyrrell, T., Turk-Kubo, K. A., Varela, M., Villareal, T. A., Webb, E. A., White, A. E., Wu, J., and Zehr, J. P.: Database of diazotrophs in global ocean: abundance, biomass and nitrogen fixation rates, *Earth System Science Data*, 4, 47–73, <https://doi.org/10.5194/essd-4-47-2012>, 2012.
- 530 Mayorga, E., Seitzinger, S. P., Harrison, J. A., Dumont, E., Beusen, A. H. W., Bouwman, A., Fekete, B. M., Kroeze, C., and van Drecht, G.: Global Nutrient Export from WaterSheds 2 (NEWS 2): Model development and implementation, *Environmental Modelling and Software*, 25, 837–853, <https://doi.org/10.1016/j.envsoft.2010.01.007>, 2010.
- Meybeck, M., Dürr, H. H., and Vörösmarty, C. J.: Global coastal segmentation and its river catchment contributors: A new look at land-ocean linkage, *Global Biogeochemical Cycles*, 20, GB1S90, <https://doi.org/10.1029/2005GB002540>, 2006.
- 535 Moore, J. K. and Doney, S. C.: Iron availability limits the ocean nitrogen inventory stabilizing feedbacks between marine denitrification and nitrogen fixation, *Global Biogeochemical Cycles*, 21, GB2001, <https://doi.org/10.1029/2006GB002762>, 2007.
- Partanen, A.-I., Keller, D. P., Korhonen, H., and Matthews, H. D.: Nutrient-enhanced productivity in the northern Gulf of Mexico: past, present and future, *Geophysical Research Letters*, 43, 7600–7608, <https://doi.org/10.1002/2016GL070111>, 2016.
- 540 Rabelais, N. N., Turner, R. E., Dortch, Q., Justic, D., Jr., V. J. B., and Jr., W. J. W.: Nutrient-enhanced productivity in the northern Gulf of Mexico: past, present and future, *Hydrobiologia*, 475/476, 39–63, <https://doi.org/10.1023/A:1020388503274>, 2002.
- Redfield, A. C., Ketchum, B. H., and Richards, F. A.: The Influence of Organisms on the Composition of Sea-Water, in: *The Sea Vol. 2*, edited by Hill, M. N., pp. 26–27, Interscience, New York, 1963.
- Ruttenberg, K. C.: The Global Phosphorus Cycle, in: *Treatise on Geochemistry*, edited by Schlesinger, W., Elsevier, <https://doi.org/https://doi.org/10.1016/B0-08-043751-6/08153-6>, 2003.
- 545 Schmittner, A., Oschlies, A., Giraud, X., Eby, M., and Simmons, H. L.: A global model of the marine ecosystem for long-term simulations: Sensitivity to ocean mixing buoyancy forcing, particle sinking, and dissolved organic matter cycling, *Global Biogeochemical Cycles*, 19, GB3004, <https://doi.org/10.1029/2004GB002283>, 2005.
- Schmittner, A., Oschlies, A., Matthews, H. D., and Galbraith, E. D.: Future changes in climate, ocean circulation, ecosystems, and biogeochemical cycling simulated for a business-as-usual CO₂ emission scenario until year 4000 AD, *Global Biogeochemical Cycles*, 22, GB1013, <https://doi.org/10.1029/2007GB002953>, 2008.
- 550 Seitzinger, S. P., Harrison, J. A., Dumont, E., Beusen, A. H. W., and Bouwman, A. F.: Sources and delivery of carbon, nitrogen, and phosphorus to the coastal zone: An overview of Global Nutrient Export from Watersheds (NEWS) models and their application, *Global Biogeochemical Cycles*, 19, GB4S01, <https://doi.org/10.1029/2005GB002606>, 2005.
- 555 Seitzinger, S. P., Mayorga, E., Bouwman, A. F., Kroeze, C., Beusen, A. H. W., Billen, G., Drecht, G. V., Dumont, E., Fekete, B. M., Garnier, J., and Harrison, J. A.: Global river nutrient export: A scenario analysis of past and future trends, *Global Biogeochemical Cycles*, 24, GB0A08, <https://doi.org/10.1029/2009GB003587>, 2010.
- Sharples, J., Middelburg, J. J., Fennel, K., and Jickells, T. D.: What proportion of riverine nutrients reaches the open ocean?, *Global Biogeochemical Cycles*, 31, 39–58, <https://doi.org/10.1002/2016GB005483>, 2017.
- 560 Sigleo, A. C. and Frick, W. E.: Seasonal variations in river discharge and nutrient export to a Northeastern Pacific estuary, *Estuarine, Coastal and Shelf Science*, 73 - Issues 3-4, 368–378, <https://doi.org/10.1016/j.ecss.2007.01.015>, 2007.
- Smith, S. V., Swaney, D. P., Talaue-McManus, L., Bartley, J. D., Sandhei, P. T., McLaughlin, C. J., Dupra, V. C., Crossland, C. J., Buddemeier, R. W., Maxwell, B. A., and Wulff, F.: Humans, Hydrology, and the Distribution of Inorganic Nutrient Loading to the Ocean, *BioScience*, 53-3, 235–245, 2003.



- 565 Somes, C. J. and Oschlies, A.: On the influence of “non-Redfield” dissolved organic nutrient dynamics on the spatial distribution of N₂ fixation and the size of the marine fixed nitrogen inventory, *Global Biogeochemical Cycles*, 29, 973–993, <https://doi.org/10.1002/2014GB005050>, 2015.
- Somes, C. J., Schmittner, A., Galbraith, E. D., Lehmann, M. F., Altabet, M. A., Montoya, J. P., Letelier, R. M., Mix, A. C., Bourbonnais, A., and Eby, M.: Simulating the global distribution of nitrogen isotopes in the ocean, *Global Biogeochemical Cycles*, 24, GB4019, <https://doi.org/10.1029/2009GB003767>, 2010b.
- 570 Somes, C. J., Oschlies, A., and Schmittner, A.: Isotopic constraints on the pre-industrial oceanic nitrogen budget, *Biogeosciences*, 10, 5889–5910, <https://doi.org/10.5194/bg-10-5889-2013>, 2013.
- Somes, C. J., Landolfi, A., Koeve, W., and Oschlies, A.: Simulating the global distribution of nitrogen isotopes in the ocean, *Geophysical Research Letters*, 43, 4500–4509, <https://doi.org/10.1002/2016GL068335>, 2016.
- 575 S  ferian, R., Berthet, S., Yool, A., Palmi  ri, J., Bopp, L., Tagliabue, A., Kwiatkowski, L., Aumont, O., Christian, J., Dunne, J., Gehlen, M., Ilyina, T., John, J. G., Li, H., Long, M. C., Luo, J. Y., Nakano, H., Romanou, A., Schwinger, J., Stock, C., Santana-Falc  n, Y., Takano, Y., Tjiputra, J., Tsujino, H., Watanabe, M., Wu, T., Wu, F., and Yamamoto, A.: Tracking Improvement in Simulated Marine Biogeochemistry Between CMIP5 and CMIP6, *Current Climate Change Reports*, 6, 95–119, <https://doi.org/10.1007/s40641-020-00160-0>, 2020.
- Townsend-Small, A., McClelland, J. W., Holmes, R. M., and Peterson, B. J.: Seasonal and hydrologic drivers of dissolved organic matter and nutrients in the upper Kuparuk River, Alaskan Arctic, *Biogeochemistry*, 103, 109–124, <https://doi.org/10.1007/s10533-010-9451-4>, 2011.
- 580 Turner, R. E., Rabelais, N. N., Justic, D., and Dortch, Q.: Global patterns of dissolved N, P and Si in large rivers, *Biogeochemistry*, 64(3), 297–317, <https://doi.org/10.1023/A:1024960007569>, 2003.
- Tyrrell, T.: The relative influences of nitrogen and phosphorus on oceanic primary production, *Nature*, 400, 525–531, 1999.
- Voss, M., Bange, H. W., Dippner, J. W., Middelburg, J. J., Montoya, J. P., and Ward, B.: The marine nitrogen cycle: recent discoveries, uncertainties and the potential relevance of climate change, *Philosophical Transactions of the Royal Society B*, 368, 20130 121, <https://doi.org/10.1098/rstb.2013.0121>, 2013.
- 585 Wang, W.-L., Moore, J. K., Martiny, A. C., and Primeau, F. W.: Convergent estimates of marine nitrogen fixation, *Nature*, 566, 205–211, <https://doi.org/10.1038/s41586-019-0911-2>, 2019.
- Weaver, A. J., Eby, M., Wiebe, E. C., Bitz, C., Duffy, P. B., Ewen, T. L., Fanning, A. F., Holland, M. M., MacFadyen, A., Matthews, H. D., Meissner, K. J., Saenko, O., Schmittner, A., Wang, H., and Yoshimori, M.: The UVic Earth System Climate Model: Model Description, Climatology, and Applications to Past, Present and Future Climates, *Atmosphere-ocean*, 39(4), 361–428, <https://doi.org/10.1080/07055900.2001.9649686>, 2001.
- 590 Westberry, T., Behrenfeld, M. J., Siegel, D. A., and Boss, E.: Carbon-based primary production modeling with vertically resolved photoacclimation, *Global Biogeochemical Cycles*, 22, GB2024, <https://doi.org/10.1029/2007GB003078>, 2008.